ABSTRACT

Title of dissertation: INSIGHTS INTO THE CONTROL OF GROWTH AND AXON GUIDANCE BY THE DROSOPHILA INSULIN RECEPTOR

Caroline Rita Li, Doctor of Philosophy, 2011

Dissertation directed by: Professor Leslie Pick
Department of Entomology

The *Drosophila* insulin receptor (DInR) regulates a diverse array of biological processes, including growth, axon guidance, and sugar homeostasis. Growth regulation by DInR is mediated by the adaptor protein Chico, the *Drosophila* homolog of vertebrate Insulin-Receptor-Substrate (IRS) proteins. In contrast, DInR regulation of photoreceptor axon guidance in the developing visual system is mediated by the SH2/SH3 domain adaptor protein Dreadlocks (Dock). In vitro studies by others suggested that different parts of DInR interact with different adaptor proteins: five NPXY motifs, one situated in the juxtamembrane region and four in the signaling C-terminal tail (C-tail), were important for interaction with Chico. Yeast two-hybrid assays suggested that a different region in the DInR C-tail interacts with Dock. To test whether these sites are required for growth or axon guidance in the animal, in vivo add-back type experiments were conducted. A panel of DInR

proteins, in which the putative Chico and Dock interaction sites had been mutated individually or in combination, were tested for their ability to rescue viability, growth, and axon guidance defects of *dinr* mutant flies. Sites important for viability were identified. In addition, mutation of all five NPXY motifs drastically decreased growth in both male and female adult flies, but did not affect photoreceptor axon guidance, showing that different binding sites on DInR control growth and axon guidance. Unexpectedly, mutation of both putative Dock binding sites, either individually or in combination, did not lead to defects in photoreceptor axon guidance. Finally, none of the seven putative ligands for DInR, the *Drosophila insulin-like peptides* (*dilps*), was required for directing photoreceptor axon guidance, although we found that *dilp1, -2, -3, -4,* and/or *-5* are required for controlling whole animal allometry. Importantly, we showed that the developmental delay exhibited by *dinr* mutants is not a factor underlying their photoreceptor axon guidance defects. Together, these studies confirmed the role of Chico-interacting regions of DInR in regulation of growth in vivo. They demonstrated that DInR is necessary to control axon guidance in vivo and showed that this role is not simply a function of developmental timing. However, they leave open the mechanisms activating DInR in regulating axon targeting.

INSIGHTS INTO THE CONTROL OF GROWTH AND AXON GUIDANCE BY THE DROSOPHILA INSULIN RECEPTOR

by

Caroline Rita Li

Dissertation submitted to the Faculty of the Graduate School of the
University of Maryland, College Park in partial fulfillment
of the requirements for the degree of
Doctor of Philosophy
2011

Advisory Committee:

Professor Leslie Pick, Chair
Professor Carol Keefer
Dr. Chi-Hon Lee
Professor Tom Porter
Professor Elizabeth Quinlan
Professor Jian Wang

Acknowledgements

Many thanks to my advisor, Dr. Leslie Pick, for her support, guidance, and encouragement throughout the years. Also, thanks to past and present members of the Pick lab for their help and input. Ray Anderson in the lab was particularly helpful in showing me how to set up the DIC optics on the lab's microscope. Thanks also to Dr. Dongyu Guo, Dr. Hua Zhang, Dr. Jingnan Liu, Julie Hou, and Pam Kaotira, who were involved in the insulin signaling projects in the lab. I would like to thank all of the members of my committee for their encouragement and advice on my graduate work. Dr. Chi-Hon Lee's advice was crucial in helping me to learn how to prepare MAb24B10-stained specimens for the photoreceptor axon guidance studies. He also provided various fly lines and he generously offered the use of, and assisted me in using, his lab's shared confocal microscope. Dr. Chun-Yuan Ting in Dr. Lee's lab also helped me with the use of the confocal microscope and generously processed the confocal images with various software. It was great that another fly lab, headed by Dr. Jian Wang, was on the same floor as, and participated in joint lab meetings with, the Pick lab, and provided fly lines and use of their lab equipment over the years. Thanks also go to Dr. Louisa Wu and her lab for providing reagents and fly lines. Finally, I would like to thank my mother, father, brother, and close friends for their support, for inspiring me, and for good times shared.

Table of Contents

List of Tables

List of Figures

List of Abbreviations

Act5C	*Actin in region 5C*
Akt1	v-akt murine thymoma viral oncogene homolog 1
arm	*armadillo*
Bl	*Bristle*
c-Cbl	Casitas B-lineage lymphoma
C-tail	C-terminal tail
CyO	*Curly of Oster*
D.	*Drosophila*
da	*daughterless*
DAB	diaminobendizine
DIC	differential interference contrast
DILP	*Drosophila* Insulin-Like Peptide
DInR	*Drosophila* insulin receptor
Dock	Dreadlocks
Dr	*Drop*
Dscam	*Drosophila* homolog of human Down syndrome cell adhesion molecule
ey	*eyeless*
FLP	Flippase, yeast site-specific recombinase
FRT	FLP recombinase target
GFP	green fluorescent protein
GMR	Glass Multimer Reporter

GOF	gain-of-function
HRP	horseradish peroxidase
Hu	Humeral
hy	hydrophobic
IGF	insulin-like growth factor
IgG	Immunoglobulin G
IPCs	insulin-producing cells
IR	Insulin Receptor
IRS	Insulin Receptor Substrate
LOF	loss-of-function
MAb	monoclonal antibody
m-NSCs	median neurosecretory cells
Msn	Misshapen
Myc	v-myc myelocytomatosis viral oncogene homolog (avian)
NCBI	National Center for Biotechnology Information
Nck	Non-catalytic region of tyrosine kinase
NGS	normal goat serum
NIK	Nck interacting kinase
OreR	OregonR
Pak	p21-activated kinase
PBS	phosphate-buffered saline
PBST	PBS containing Tween 20
PBT	PBS containing Triton-X-100

PC	prohormone convertase
PH domain	pleckstrin homology domain
PI3K	phosphatidylinositol 3-kinase
PKB	protein kinase B
PTB domain	phosphotyrosine binding domain
pY	phosphorylated tyrosine
R cells	photoreceptor cells or photoreceptors
RFP	red fluorescent protein
RNAi	RNA interference
Robo	Roundabout
ry	*rosy*
Sb	Stubble
SH2 domain	Src Homology 2 domain
SH3 domain	Src Homology 3 domain
Sp	*Sternopleural*
Tb	Tubby
Tor	Target of rapamycin
UAS	upstream activation sequence
w^{1118}	*white*^{1118}
WT	wild type

Chapter 1: Introduction

1.1 Insulin receptor structure and signaling in mammals and *Drosophila*

The mammalian insulin receptor (IR) is a receptor tyrosine kinase composed of two extracellular α subunits (135 kDa each) and two transmembrane β subunits (95 kDa each). This tetramer is a constitutively disulfide-linked glycoprotein. The β subunits possess tyrosine kinase activity that is repressed by the α subunits. Ligand-binding to the α subunits leads to a conformational change that relieves the repression of β subunit tyrosine kinase activity. The β subunits then autophosphorylate, causing another conformational change, which produces an additional increase in kinase activity (reviewed in Kohanski, 2002; Saltiel and Kahn, 2001). Tyrosine residues of several docking proteins, such as the four Insulin-Receptor Substrate (IRS) proteins, are phosphorylated by the activated insulin receptor. The phosphorylated tyrosines on IRS serve as binding sites for SH2 domain-containing proteins. Thus, the docking proteins can recruit SH2 domain-containing adaptor proteins and enzymes, such as the phosphatidylinositol 3-kinase (PI3K) regulatory subunit p85. The overall effect of insulin receptor activation is the launching of multiple downstream signaling pathways that control diverse processes such as cell growth, cell proliferation, glucose homeostasis, fertility, and aging (reviewed in Dickson, 2003; Saltiel and Kahn, 2001; White, 2006)(Figure 1).

The *Drosophila insulin receptor* (*dinr)* gene was isolated by screening a *Drosophila* genomic library with a human insulin receptor fragment containing sequences encoding the insulin binding and kinase domains (Petruzzelli et al., 1986).

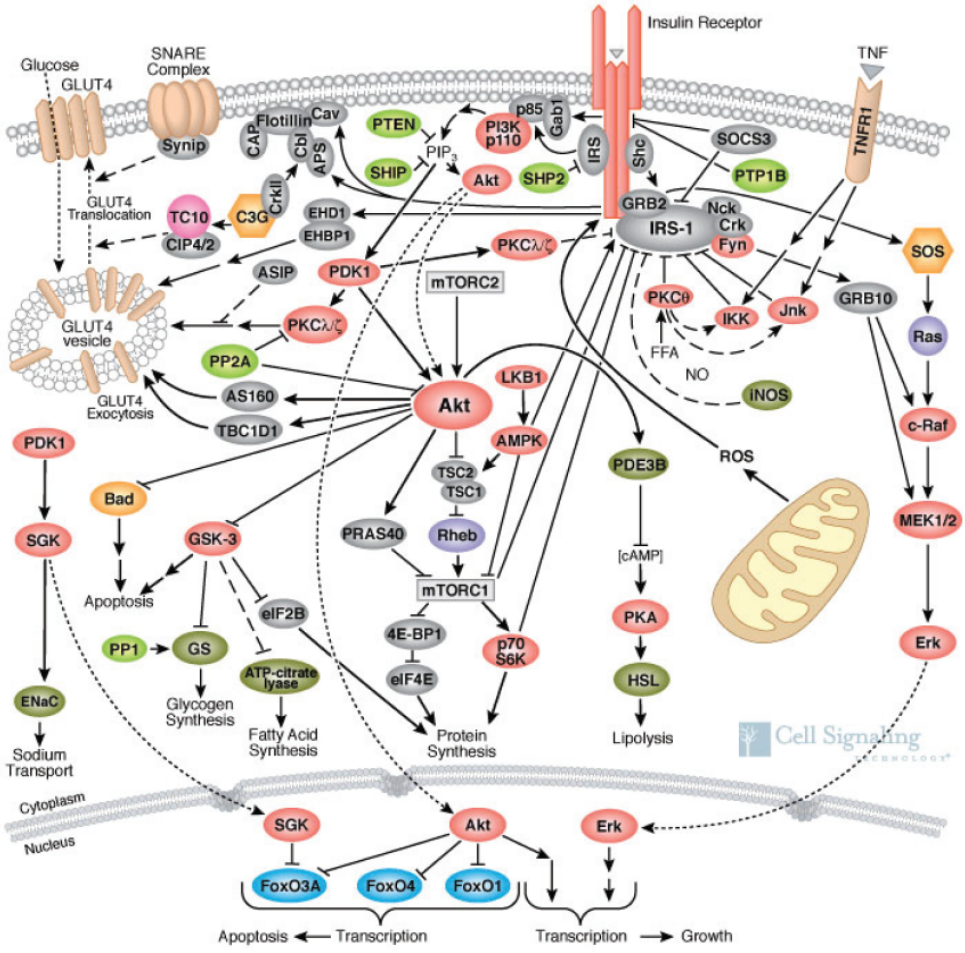

Figure 1. Multiple signaling pathways lie downstream of the mammalian insulin receptor. The mammalian IR uses different downstream pathways to control cellular processes such as growth and glucose uptake. Many of the downstream pathways overlap with each other. Pathway diagram reproduced courtesy of Cell Signaling Technology, Inc. (www.cellsignal.com).

DInR autophosphorylated in cell culture in response to porcine insulin (Fernandez-Almonacid and Rosen, 1987). Unlike the mammalian insulin receptor, which binds insulin with high affinity and IGF1 and IGF2 with low affinity (reviewed in Kohanski, 2002), DInR was activated only by insulin (Fernandez-Almonacid and Rosen, 1987). Structurally, DInR is considerably similar to human IR (26.3% overall identity, as calculated using the MatGAT program (Campanella et al., 2003)), particularly in the kinase domain, which is 65% identical (Fernandez et al., 1995). However, the DInR β subunit contains a 60 kDa C-terminal extension (C-tail), not present in the mammalian insulin receptor, that harbors potential SH2 domain binding sites proposed to confer IRS1-like function (Fernandez et al., 1995; Ruan et al., 1995; reviewed in Yamaguchi et al., 1995). Our lab found that Dock, the *Drosophila* homolog of mammalian Nck, binds directly to the C-tail of DInR (Song et al., 2003)(Figure 2 and 3), while mammalian Nck is recruited to IR via an interaction with IRS1 rather than IR itself (Lee et al., 1993)(Figure 1). *Drosophila* Chico, a homolog of mammalian IRS1-4, is thought to act downstream of DInR to regulate growth through the PI3K-Akt/PKB signaling pathway (Bohni et al., 1999; reviewed in Dickson, 2003)(Figure 2). Since there is only one IRS homolog in *Drosophila*, compared to the four main IRS family members in mammals, and only one Nck homolog in *Drosophila*, compared to the two Nck homologs in humans, it appears that downstream IR signaling is less complex in *Drosophila.* Thus, untangling the signaling mechanisms used by the insulin receptor to control its different downstream functions would be expected to be more tractable using the *Drosophila* model system.

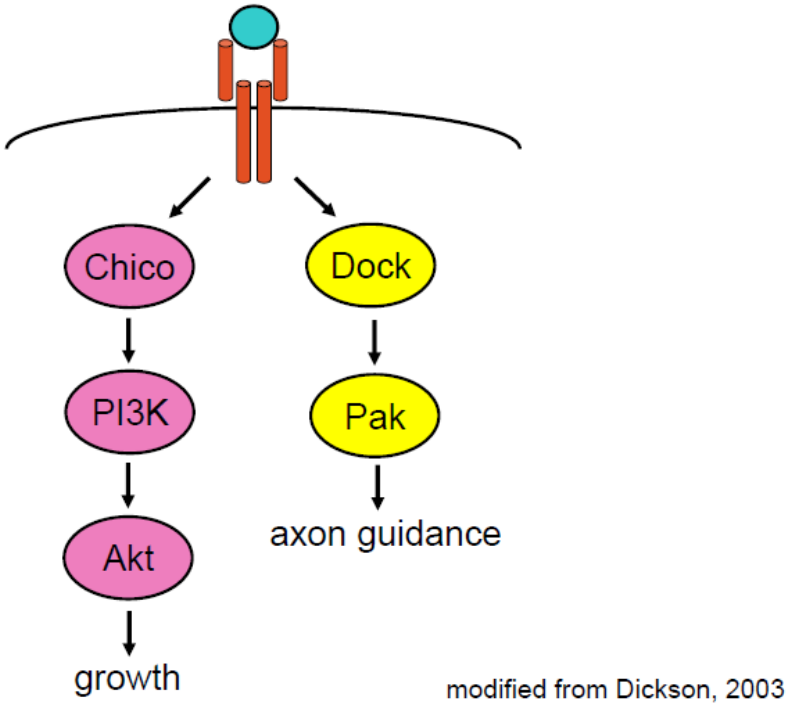

Figure 2. Model for DInR control of growth and photoreceptor axon guidance. We and others proposed that DInR regulates diverse biological functions via interaction with different adaptor proteins that initiate different downstream pathways. Presumably upon binding its ligand(s) (blue circle), DInR (orange tetramer) autophosphorylates and recruits adaptor proteins. Chico connects DInR to the PI3K-Akt signaling pathway for growth control, whereas Dock connects DInR to the Pak signaling pathway for photoreceptor axon guidance control. Figure was modified from Dickson, 2003.

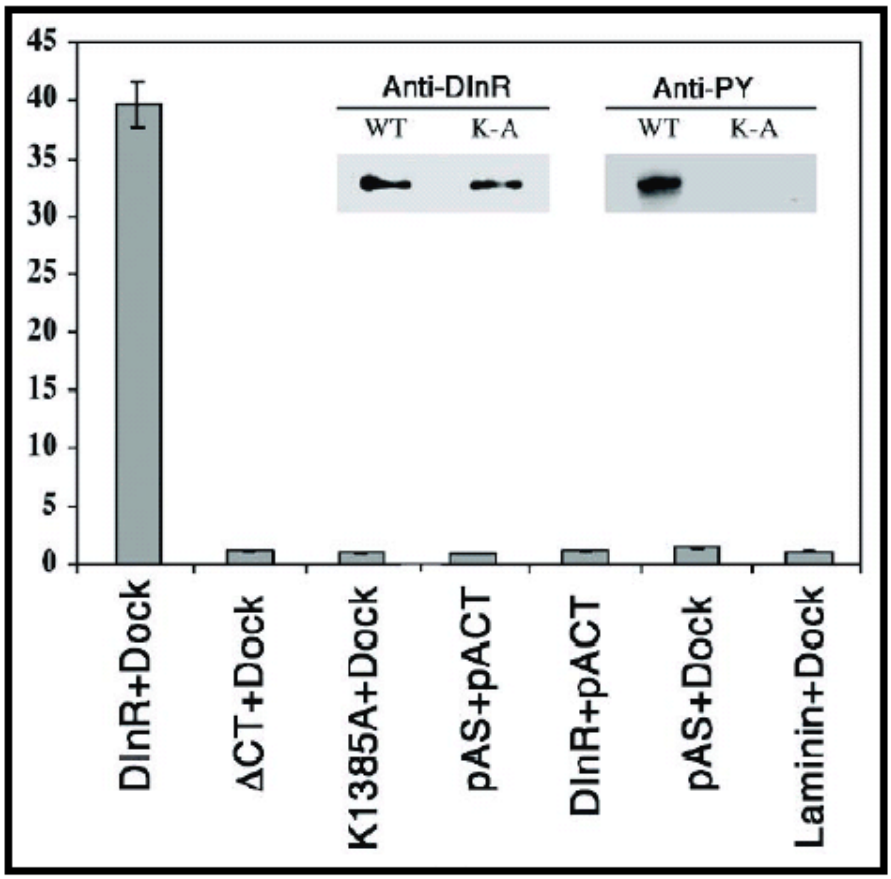

from Song et al., 2003

Figure 3. A yeast two-hybrid screen for proteins that interact with the intracellular domain of DInR identified Dock. DInR and Dock interacted in a yeast two-hybrid screen. This interaction depended on the C-tail of DInR since deletion of the C-tail (ΔCT) abolished binding with Dock. DInR and Dock binding also depends on the autophosphorylation of DInR since a kinase-dead mutant DInR protein (K1385A) failed to bind Dock. The last four bars in the graph are negative controls. The insets show Western blots of extracts from

yeast expressing the DInR intracellular domain (WT) or the kinase-dead DInR (K-A). The left inset was stained with an anti-DInR antibody, showing that both wild type and kinase-dead receptors were expressed in yeast. The right inset was stained with a phosphotyrosine antibody, confirming the lack of autophosphorylation by kinase-dead DInR in the yeast system. Figure from Song et al., 2003.

1.2 Insulin and the *Drosophila* insulin-like peptides

Mammalian preproinsulin is composed of four domains: the signal peptide, the B-chain, the C-chain, and the A-chain, which are transcribed in this order. Cleavage of the signal peptide from preproinsulin inside the lumen of the rough endoplasmic reticulum yields proinsulin. Proinsulin is then converted within acidifying secretory granules into C-peptide and insulin, which consists of the B-chain and the A-chain joined together by disulfide bonds. Three enzymes are responsible for this conversion: prohormone convertase 1/3 (PC1/3), prohormone convertase 2 (PC2), and carboxypeptidase H/E. Each of these enzymes has multiple substrates besides insulin (Bailyes et al., 1992; Bennett et al., 1992; reviewed in Leiter, 1997; Shoelson and Halban, 1994; Steiner, 1998). The *Drosophila* homolog of PC2, *amontillado*, has been identified (Siekhaus and Fuller, 1999).

In the 1970s, documentation of the presence of insulin-like substances in invertebrates such as *Drosophila* began appearing in the literature (reviewed in LeRoith et al., 1981). Even more surprisingly, insulin-like material was also found in unicellular organisms, such as *Tetrahymena pyriformis*, a ciliated protozoan, and *Neurospora crassa*, a fungus, thus indicating the evolutionarily ancient origins of the molecule. Le Roith et al. (1981) identified insulin-like material in extracts from *Drosophila* heads and bodies using both an insulin bioassay and an insulin radioimmunoassay. The insulin radioimmunoassay used was considered to be a stringent test of a substance's structural similarity to insulin, since the A-chain and the B-chain must be joined by disulfide bridges in order to yield a positive result in the assay (reviewed in Le Roith et al., 1981).

The completion of the *Drosophila melanogaster* genome sequence in 2000 (Adams et al., 2000) facilitated the search for insulin-like genes in this organism. Seven *Drosophila insulin-like peptides* (*dilps*) were identified in the *Drosophila* genome by computational searches conducted by Brogiolo et al. (2001). The *dilp1*, *-2, -3, -4,* and *-5* genes are located in a cluster on the third chromosome. The *dilp6* and *dilp7* genes are present at different loci on the X chromosome. The criteria used for the initial computational search was the conserved spacing of the four cysteine residues found in the human insulin A-chain. This led to the identification of *dilp2*. The predicted *Drosophila* A-chain of *dilp2* was then used to identify the six other *dilps*. There are two major reasons why the *dilps* are thought to encode insulin molecules, not insulin-like growth factors (IGFs). First, the predicted mature DILP peptides share a higher percentage of amino acid identity with mature human insulin than with mature IGF1 or IGF2. For example, the predicted mature DILP2 peptide shares an amino acid identity of 35% with mature human insulin, 26% with mature human IGF1, and 28% with mature human IGF2. Second, although the IGFs also contain four cysteine residues in their A-chains, they lack the proteolytic cleavage sites between the A-, B-, and C-chains, which are present in human insulin and in the predicted structures of DILP1, -2, -3, -4, -5, and -7. The predicted structure of DILP6 lacks the proteolytic cleavage site between the B-chain and C-chain, suggesting it may be more IGF-like (Brogiolo et al., 2001).

Human insulin is best known for its role in glucose homeostasis and for its absence in patients suffering from type 1 diabetes (reviewed in Gale, 2001; Pessin and Saltiel, 2000). The islets of Langerhans in the pancreas contain β-cells that

produce insulin (reviewed in Ramiya et al., 2000). Clusters of cells in the *Drosophila* brain called the median neurosecretory cells (m-NSCs) or insulin-producing cells (IPCs) express *dilp1, -2, -3,* and *-5* mRNA (Brogiolo et al., 2001; Rulifson et al., 2002). The m-NSCs are thought to be analogous to the vertebrate β-cells because increased levels of carbohydrates in the larval hemolymph were observed when the m-NSCs were ablated (Rulifson et al., 2002), and because expression of some *dilps*, *dilp3* and *dilp5*, in these cells was nutrient-responsive (Ikeya et al., 2002).

In situ hybridizations showed that the seven *dilp* genes are expressed in various patterns, sometimes overlapping, in embryos and larvae (Brogiolo et al., 2001). Some, as mentioned above, are expressed in brain IPCs, while others are expressed in the embryonic mesoderm (*dilp4* at high levels earlier in development; *dilp2* at low levels later in development), embryonic anterior midgut rudiment (*dilp4*), embryonic midgut (*dilp2* at high levels; *dilp7* at moderate levels), larval salivary glands (*dilp2*), larval midgut (*dilp4*), larval gut (*dilp5* at moderate levels; *dilp6* at low levels), and ten specific cells in the larval ventral nerve cord (*dilp7*)(Brogiolo et al., 2001).

Despite these RNA expression profiles, the tissue targets and sites of action of each DILP protein may be different than the sites of RNA expression, since these peptides are expected to be secreted. To our knowledge, the localization of peptides in vivo has only been examined thus far for DILP2, DILP3, DILP4, and DILP5, using peptide-specific antibodies. In larvae, DILP2 and DILP5 are found in the cell bodies and axonal projections of the brain IPCs, and their axonal termini on the aorta and corpora cardiaca (Geminard et al., 2009; Rulifson et al., 2002). Another place

where DILP2 has been observed in larvae is in the surface glial cells in the thoracic ventral nerve cord (Chell and Brand, 2010). In adults, DILP2, DILP3, and DILP5 have been observed in the brain IPCs (Gronke et al., 2010). DILP4 has been observed in a widespread pattern in neurons of the adult brain (Gronke et al., 2010).

1.3 Roles of insulin signaling in viability, growth, and physiology

DInR has been shown to be required for viability (Fernandez et al., 1995), growth (Chen et al., 1996; Fernandez et al., 1995), female fertility (Chen et al., 1996), and normal lifespan (Tatar et al., 2001). DInR also controls developmental timing, since certain viable heteroallelic combinations of *dinr* alleles gave rise to animals that were severely developmentally delayed (Chen et al., 1996). The *dilps* that control the functions stated above for DInR have recently been identified. Viability relies on *dilp2*, *-3, -5,* and *-6*, since loss of these *dilps* together caused complete lethality (Gronke et al., 2010). Larval growth appears to be mainly controlled by *dilp2, -3,* and *-5* (Gronke et al., 2010), whereas pupal growth is controlled by *dilp6* (Slaidina et al., 2009). Both female fertility and developmental timing seem to depend on *dilp2, -3, -5,* and *-6* (Gronke et al., 2010). The loss of *dilp2* led to an increased lifespan; thus it is required for normal lifespan (Gronke et al., 2010).

Insulin signaling has been shown to regulate sugar levels in *Drosophila*. In many insects, trehalose, a disaccharide made up of two glucose molecules, is the main circulating sugar in the hemolymph (reviewed in Rulifson et al., 2002); hemolymph is the insect equivalent to blood. Rulifson et al. (2002) saw an increase in combined trehalose and glucose levels in larval hemolymph when they ablated the insulin-

producing cells (IPCs) in the brain by expressing Reaper, a cell death-promoting factor, under the control of the *dilp2* promoter. These results were consistent with *dilp1, -2, -3,* and/or *-5*, the *dilps* that are expressed in the IPCs, as being involved in regulating sugar levels in larval hemolymph; however, the results were not conclusive because the IPCs likely produce other candidate hormones for sugar homeostasis besides the *dilps*. Our group showed that combined trehalose and glucose levels in larval and adult male hemolymph are abnormally elevated in a mutant lacking *dilp1, -2, -3, -4,* and *-5* (Zhang et al., 2009). Broughton et al. (2008) knocked down *dilp2* levels using *dilp2* RNAi driven by a portion of the *dilp2* promoter, but saw no effect on the levels of trehalose and glucose in the hemolymph of fasting larvae and adults. This result does not necessarily rule out the involvement of *dilp2* in controlling hemolymph sugar levels since *dilp2* might be acting redundantly with another *dilp*. Thus, taken together with the results of Zhang et al. (2009), it is still not known whether all or a subset of the *dilp1, -2, -3, -4,* and *-5* genes are required for regulating hemolymph sugar levels.

For adults in which *dilp2* RNAi was driven by part of the *dilp2* promoter, Broughton et al. (2008) did observe an increase in the levels of whole body trehalose, which is thought to reflect trehalose that has been stored. More recently, single and combination null mutants of the *dilp* genes were generated (Gronke et al., 2010). Adult *dilp2* mutant flies showed an increase in stored trehalose levels (Gronke et al., 2010), thus confirming the *dilp2* RNAi results obtained by Broughton et al. (2008). Adult *dilp3* and *dilp5* single mutants had normal stored trehalose levels (Gronke et al., 2010); these mutants in particular were tested because it was previously observed

that the knockdown of *dilp2* by RNAi led to a compensatory increase in *dilp3* and *dilp5* mRNA levels (Broughton et al, 2008). Other *dilp* mutants were not tested for trehalose storage (Gronke et al., 2010). Another component of the insulin signaling pathway, the insulin receptor, has also been implicated in controlling trehalose storage. Belgacem and Martin (2006) observed abnormally high adult whole body trehalose levels in the *dinr* mutant heterozygotes and transheterozygotes that they examined.

Since DInR is pleiotropic, the interplay between the various functions of this receptor is an interesting problem. Evidence suggests that the use of one receptor for different downstream functions may be a mechanism for synchronizing some of these functions. Using a mutant clone approach, Bateman and McNeill (2004) showed that DInR acts through PI3K and Tor to control the timing of differentiation of neurons in the eye and leg imaginal discs. Since DInR is also involved in controlling growth, it can thus couple the pace of differentiation to that of growth, in order to achieve proper tissue patterning. In contrast, other evidence indicates that DInR can control some of its functions in an uncoupled manner. For example, the control of photoreceptor axon guidance by DInR occurs through the downstream Dock signaling pathway, and appears to be independent of the control of growth by DInR through the downstream Chico signaling pathway, since *chico* mutants did not exhibit the photoreceptor axon guidance defects seen in *dinr* mutants (Song et al., 2003).

1.4 Downstream of insulin signaling: adaptor proteins

Adaptor proteins act as linkers between different parts of signaling pathways,

such as activated cell-surface receptors and downstream effector proteins (reviewed in Pawson, 2007). The structural composition of adaptor proteins reflects their narrowly defined role; adaptor proteins are solely made up of interaction domains and motifs.

Docking proteins are adaptor proteins that contain docking sites for other adaptor proteins; they serve as a means of signal amplification for receptors (reviewed in Pawson and Scott, 1997). Docking proteins usually consist of 1) an N-terminal membrane-targeting element, which can be a pleckstrin homology (PH) domain or a myristylation site, 2) a phosphotyrosine binding (PTB) domain that interacts with the receptor's NPXY autophosphorylation site, and 3) a series of tyrosine phosphorylation sites that become phosphorylated by the activated receptor and that then allow recruitment of effector proteins through their SH2 domains (reviewed in Brummer et al., 2010; Lemmon and Schlessinger, 2010; Pawson and Scott, 1997).

The insulin receptor substrate (IRS) family contains primarily four members, IRS1-4, which act as docking proteins for the insulin and IGF1 receptors (reviewed in Pawson and Scott, 1997 and Lemmon and Schlessinger, 2010). IRS5 and IRS6 are also sometimes considered to be part of the IRS family, but they are more distantly related to IRS1-4, their C-termini are truncated in comparison, and their phosphorylation in response to insulin is weaker (Brummer et al., 2010). IRS1, the prototypical and most well-characterized member of the IRS family, contains over twenty potential tyrosine phosphorylation sites; nine of these sites are located within YXXM motifs that are the preferred binding sites for SH2 domains of the PI3K p85

subunit (Brummer et al., 2010). The activation of PI3K is the best-studied pathway downstream of IRS1. Chico is the *Drosophila* homolog of the mammalian IRS proteins (Bohni et al., 1999). It is not known whether Chico regulates circulating sugar levels in *Drosophila*, although the IRS proteins are known to regulate glucose levels in mammals. Chico will be discussed in more detail in Chapter 6.

The Nck family of adaptor proteins contains two members in humans and mice (reviewed in Buday et al., 2002; Fawcett et al., 2007). Nck is composed exclusively of one SH2 domain and three SH3 domains. Nck often links to effector molecules that are involved in regulating the actin cytoskeleton (reviewed in Li et al., 2001). It was recently found in mice that Nck is involved in axon guidance and in organizing neuronal circuits that are used for limb movement (Fawcett et al., 2007). The *Drosophila* homolog of Nck is Dreadlocks (Dock)(Garrity et al., 1996), which will be discussed further in Chapter 6.

SH2B proteins are adaptor proteins that contain a PH domain, an SH2 domain, multiple tyrosine and serine/threonine phosphorylation sites, an N-terminal proline-rich region, and a C-terminal c-Cbl recognition motif (reviewed in Slack et al., 2010). Mammals have 3 SH2B family members, which have roles in glucose homeostasis, energy metabolism, reproduction, and hematopoesis. There is only one SH2B homolog, called Lnk, in *Drosophila melanogaster*. Lnk was shown to act in parallel with Chico to control cell growth and proliferation in *Drosophila* (Werz et al., 2009). Lnk was also shown to act downstream of DInR and upstream of PI3K during growth control by genetic epistasis experiments (Werz et al., 2009). It is not known whether Lnk binds directly to DInR. If it does, it would be interesting to determine whether

the SH2 domain of Lnk could potentially mediate direct interaction with DInR through one of the ten tyrosine phosphorylation sites in the C-tail of DInR. Lnk has also been implicated in the control of lifespan, oxidation resistance, and starvation resistance (Slack et al., 2010).

1.5 Photoreceptor axon guidance in *Drosophila*

1.5.1 General mechanisms

Many axons must traverse large distances that can sometimes be greater than a thousand times the length of a neuronal cell body (reviewed in Tessier-Lavigne and Goodman, 1996). A special structure at the leading edge of an axon is the growth cone. The growth cone is responsible for sensing and responding to guidance cues in the surrounding environment (reviewed in Huber et al., 2003). There are four basic ways by which extracellular cues can influence growth cone behavior: 1) contact attraction, 2) contact repulsion, 3) chemoattraction, and 4) chemorepulsion. Contact attraction and repulsion are mediated by extracellular matrix and cell surface molecules that do not diffuse. Chemoattraction and chemorepulsion are mediated by diffusible factors, some of which may form gradients (reviewed in Tessier-Lavigne and Goodman, 1996). The ultimate effect of extracellular cues is a change in the cytoskeleton of axonal growth cones. This can lead to the advancement or retraction of the growth cones (reviewed in Huber et al., 2003).

1.5.2 The *Drosophila* visual system

Each adult compound eye of *Drosophila melanogaster* contains

approximately 750 ommatidia. Each ommatidium in turn is composed of eight different photoreceptors (R cells) that are referred to as R1 to R8 (reviewed in Tayler and Garrity, 2003). The differentiation of photoreceptor neurons and the assembly of ommatidia occur in the epithelium of the eye imaginal discs of larvae and pupae. Photoreceptor differentiation and ommatidial assembly occur in a row-by-row fashion, starting from the posterior of each eye imaginal disc during the third-instar larval stage and finishing at the anterior of each eye imaginal disc during the early pupal stage (reviewed in Kunes et al., 1993)(Figure 4).

As a row of differentiated photoreceptors forms, the photoreceptors of that row send their axons through the ipsilateral optic stalk and then into the ipsilateral optic lobe in a roughly synchronized manner (reviewed in Kunes et al., 1993). The axons of R1-6 neurons are targeted to the lamina, which is the most superficial optic ganglion in the brain (reviewed in Tayler and Garrity, 2003)(Figure 4). Glial cells, not lamina neurons, are required for R1-6 targeting (Poeck et al., 2001). The R7 and R8 axons are targeted to different layers of the medulla, which is an optic ganglion underlying the lamina (reviewed in Tayler and Garrity, 2003)(Figure 4). Correct targeting is important because each class of photoreceptors carries different visual information; R1-6 cells detect green or blue light, R7 cells detect UV light, and R8 cells detect blue light (reviewed in Mast et al., 2006).

The layer-specific targeting of axons is just one aspect of the specificity of photoreceptor axon targeting. Another is topographic map formation in both the medulla and the lamina. The medullar topographic map is easily seen in wild type eye-brain complexes (Figure 4). Growth cones terminate in a regular staggered

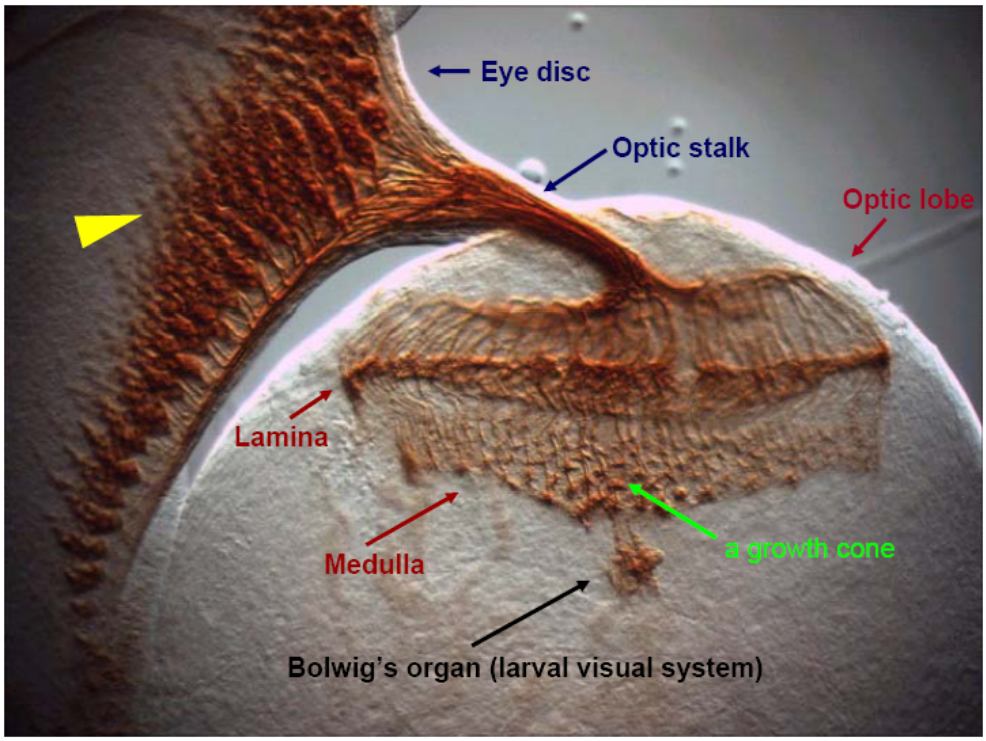

Figure 4. Topographic map of the developing adult visual system. Photoreceptor (R-cell) axon targeting from the developing eye imaginal disc to the brain was revealed by immunostaining with the monoclonal antibody 24B10, which stains differentiated photoreceptors and their axons. During development of the adult visual system, which starts to occur during the third-instar larval stage, rows of photoreceptors differentiate starting from the posterior of the eye disc and ending at the anterior. This specimen has approximately eleven rows of differentiated photoreceptors. The yellow arrowhead indicates where the newest row of differentiated photoreceptors was

added. The differentiated photoreceptors send their axons through the optic stalk to the optic lobe of the brain. Axons from photoreceptors R1-6 terminate in the lamina layer of the optic lobe, forming a smooth-appearing pattern, whereas axons from R7 and R8 cells terminate in the medulla layer, forming a staggered pattern with their growth cones. The Bolwig's organ is part of the larval visual system.

pattern in the medulla. Visual input does not play a role in establishing the topographic maps since synapses between photoreceptor axons and their targets will form later in development. Each synaptic unit in a topographic map will relay information about a single point in visual space. Thus, it is important that the relative positions of the photoreceptor neuron cell bodies in the eye are maintained by their axons at targets in the optic lobe (reviewed in Clandinin and Zipursky, 2002; Lee et al., 2001; Prokop and Meinertzhagen, 2006).

Much has been learned about the cellular and molecular mechanisms that are involved in guiding *Drosophila* photoreceptor axons to their targets. One key molecule involved in axon guidance is Dreadlocks (Dock), which is an SH2/SH3 adaptor protein with 43% overall identity to the human Nck protein. Dock was identified in a screen for mutants with photoreceptor axon guidance defects (Garrity et al., 1996). Dock can be recruited by different upstream signaling molecules in different areas of the nervous system. For example, DInR recruits Dock in adult photoreceptor axons (Song et al., 2003). In contrast, Dscam is thought to recruit Dock in the Bolwig's nerve, which is a component of the larval visual system (Schmucker et al., 2000). Also, at the embryonic central nervous system midline, the Robo receptor recruits Dock (Fan et al., 2003). Dock is upstream of at least two signaling pathways in photoreceptor axons. One of the pathways contains p21-activated kinase (Pak), while the other contains Misshapen (Msn), the *Drosophila* homolog of Nck interacting kinase (NIK). Pak and Msn are both Ste20-like serine/threonine kinases, but they belong to different families (Hing et al., 1999; reviewed in Rao, 2005; Ruan et al., 1999; Su et al., 2000).

1.5.3 A role for DInR in photoreceptor axon guidance

A novel role for DInR, in regulating photoreceptor axon guidance through the Dock-Pak signaling pathway, was discovered by Song et al. (2003). A yeast two-hybrid screen was conducted using the intracellular domain of DInR as bait in order to identify potential signaling molecules immediately downstream of DInR. Dock was one of the molecules that showed an interaction with DInR (Figure 3). This interaction was dependent on DInR kinase activity (Figure 3). Deletion of the DInR C-tail abolished the interaction between DInR and Dock, showing that the C-tail is *necessary* for the interaction (Figure 3). However, it is not known whether the C-tail is *sufficient* for DInR and Dock binding. The SH2 and SH3 domains of Dock were shown to be required for interaction with DInR, using yeast two-hybrid assays. Co-immunoprecipitation experiments, using lysates from wild type adult flies, confirmed that DInR and Dock interact in vivo in a stable complex. In addition, both Dock (Garrity et al., 1996; Hing et al., 1999) and DInR protein (Song et al., 2003) localize to photoreceptor axons and growth cones. The FLP/FRT system for mosaic analysis (Golic, 1991; Xu and Rubin, 1993), with an eye-specific driver for *FLP* (*eyFLP*)(Newsome et al., 2000), was used to test the role of DInR in axon guidance in vivo. DInR was indeed required in photoreceptors for proper axon guidance to take place during the third-instar larval stage, as the *dinr* mutant eye mosaics displayed abnormal gaps and clumps in their photoreceptor axon targeting pattern and also showed a failure of growth cones in the medulla to expand (Song et al., 2003). *dinr* mutant transheterozygotes were also observed to have abnormal gaps and clumping in their axonal projection pattern. Furthermore, DInR is required in photoreceptors for

the targeting of R7 and R8 growth cones to the correct layers in the adult optic lobe. Genetic interaction experiments showed that DInR acts through Dock, not Chico, to guide photoreceptor axons. Consistent with this finding was the lack of photoreceptor axon guidance defects in *chico* mutants (Song et al., 2003).

Recently, it was found in mammalian cell culture that insulin signaling regulates normal axon cone morphology and organization of the actin cytoskeleton in developing photoreceptors (Rajala et al., 2009). It would be worthwhile to determine whether insulin signaling controls photoreceptor axon development in mammals through similar downstream signaling mechanisms as in the invertebrate *Drosophila melanogaster*.

1.6 Other roles for insulin signaling in the development and function of the nervous system

Although the mammalian brain was once considered an "insulin-insensitive" organ, recent evidence indicates otherwise (reviewed in Chiu and Cline, 2010). In mammals, insulin signaling has been shown in neuronal cell culture experiments to regulate dendritic spine density and neurite outgrowth. Insulin signaling has also been implicated in neuronal survival, synaptic plasticity, learning and memory, and neurological disorders. IGF signaling is known to be involved in various processes in neuronal development, such as growth cone expansion, axon outgrowth, and neuronal polarity (reviewed in Scolnick et al, 2008). IGF signaling was recently shown to be involved in axon guidance and sensory map formation in the developing olfactory system of mice (Scolnick et al., 2008).

Evidence indicating roles for insulin signaling in the nervous system of flies, other than in photoreceptor axon guidance (discussed in the previous section), has also accumulated. In *dinr* mutant embryos, various defects were observed in the developing central and peripheral nervous systems (Fernandez et al., 1995).

Insulin signaling is involved in the nutrition-dependent exit from quiescence of neural stem cells (called neuroblasts in *Drosophila*) in the thoracic ventral nerve cord (Chell and Brand, 2010). Dietary amino acids are sensed by the fat body (Britton and Edgar, 1998), which then induces *dilp2* and *dilp6* expression in the surface glia that neighbor the neuroblasts (Chell and Brand, 2010); in a paracrine fashion, *dilp2* and *dilp6* then activate the DInR-PI3K-Akt pathway in the neuroblasts to cause cell growth and proliferation.

Although DInR expression has been found at the neuromuscular junctions of *Drosophila* larvae (Gorczyca et al., 1993), it is not clear whether insulin signaling plays a role there in regulating synaptic development or physiology. Since the absence of zygotic Dock in embryos has been shown to delay synapse formation by the RP3 motoneuron (Desai et al., 1999), it would be interesting to test whether DInR interacts with Dock in this process too.

Murillo-Maldonado et al. (2011) found evidence suggesting that insulin signaling is required for normal neuronal communication involving two different neurotransmitters. Electroretinograms, a method of measuring retinal physiology, were recorded for various insulin pathway mutants. It was found that some of the mutants had defects in retinal function, which relies on histamine, the neurotransmitter in fly photoreceptors. In addition, cholinesterase activity in fly head

extracts from some of the insulin pathway mutants was abnormally low, thus indicating that the metabolism of acetylcholine, which is the major excitatory neurotransmitter in fly brains, was impaired.

Chapter 2: Materials and Methods

2.1 Molecular biology and generation of transgenic flies

To test rescue of *dinr*-associated mutant phenotypes, *dinr* cDNAs which were full-length or partial, or which carried specific mutations, were inserted into the expression vector pUAST-Myc, which includes a 102 bp region encoding a 3X Myc tag, to generate in-frame C-terminal fusions. To generate *UAS-dinr(JM-NPFF)-myc3*, the tyrosine in the juxtamembrane NPFY motif of *UAS-dinr-myc3* was changed to a phenylalanine. Site directed mutagenesis to change the TAT codon for tyrosine to the TTT codon for phenylalanine was carried out with standard methods using a *dinr* cDNA in a pSP vector (*pSP-dinr-myc3*) and Vent polymerase (NEB), and was verified by sequencing. A ~7 kb fragment spanning the entire *dinr-myc3* coding region, and thus containing the mutated juxtamembrane NPFF site, was released from the *pSP-dinr-myc3* plasmid with NotI and EcoRI; the fragment was then inserted into the NotI and EcoRI sites of *UAS-dinr(Y,7,8,9,10F)-myc3*, replacing the entire *dinr(7,8,9,10F)-myc3* coding region.

UAS-dinr(5NPXF)-myc3 was made by excising a ~4 kb fragment containing the 4 mutated NPXF sites in the C-tail from *UAS-dinr(Y7,8,9,10F)-myc3* using AflII and inserting it into the AflII site of *pUAST-dinr(JM-NPFF)-myc3* to replace the AflII fragment. Orientation of the insert was verified by sequencing.

The *UAS-dinr(JM-NPFF)-myc3* and *UAS-dinr(5NPXF)-myc3* constructs were injected into w^{1118} embryos by Rainbow Transgenic Flies, Inc. (California) in order to generate transgenic flies by P-element-mediated transformation. Twelve independent

transformant lines were obtained from Rainbow Transgenic Flies, Inc. for *UAS-dinr(JM-NPFF)-myc3*, whereas nine independent lines were obtained for *UAS-dinr(5NPXF)-myc3*. I used standard methods to balance the insertions over *CyO* (for insertions on the second chromosome) or *TM3Sb* (for insertions on the third chromosome). For the *dinr* mutant rescue experiments, only insertions on the second chromosome were ideal for use. Four *UAS-dinr(JM-NPFF)-myc3* lines were found to have insertions on the second chromosome. Only one *UAS-dinr(5NPXF)-myc3* line was found to have an insertion on the second chromosome.

2.2 Fly stocks and genetics

The following genetic crossing schemes were followed to generate stocks for the rescue experiments performed in Chapter 6. *UAS-dinr* transgenes are indicated as "*UAS-X*" in this description. *Sp/CyO;Dr/TM3Sb,armGFP* virgin females were crossed to a single male carrying a *UAS-X* transgene on the second chromosome. To double balance, male or virgin female *CyO, Dr* progeny flies were crossed to male or virgin female (as the case required) *CyO, Sb* progeny flies. The resulting progeny that carried both *Dr* and *Sb* were crossed to each other to generate *UAS-X/(UAS-X* or *CyO);Dr/TM3Sb,armGFP* stocks that were maintained. Males from this stock were then crossed to *Sp/CyO;dinr^{ex15}/TM3Sb,armGFP* virgin females. Non-*Sp*, *CyO*, non-*Dr* progeny were self-crossed to yield *UAS-X/(UAS-X* or *CyO);dinr^{ex15}/ TM3Sb,armGFP* stocks to be used for adult assays. To generate the stocks to be used for larval assays, *Bl/CyO,GFP;TM3Sb/TM6BTb,GFP* virgin females were crossed to *UAS-X/(UAS-X* or *CyO);dinr^{ex15}/TM3Sb,armGFP* males. Non-*Bl*, non-*Sb*, *Hu* (an

adult marker on the *TM6BTb,GFP* balancer) progeny were self-crossed to generate *UAS-X/*(*UAS-X* or *CyO,GFP*)*;dinr*^{ex15}*/TM6BTb,GFP* stocks.

For the lethality rescue analysis, *arm-GAL4/arm-GAL4; FRT82Bdinr*^{273}*/ TM3Sb,armGFP* virgin females were crossed to *UAS-X/(UAS-X* or *CyO); dinr*^{ex15}*/ TM3Sb,armGFP* males. Parental flies were removed as necessary to prevent overcrowding of progeny. Adult progeny of each genotype that had eclosed were scored for their bristle phenotype: either Sb or non-Sb. In the case that the *UAS-X* construct to be tested was homozygous lethal and had to be used in crosses with a *CyO* balancer, only non-*CyO* eclosed adult progeny were scored for their bristle phenotype.

For the growth defect rescue analysis, *arm-GAL4/arm-GAL4;FRT82Bdinr*^{273}*/ TM3Sb,armGFP* virgin females were crossed to *UAS-X/(UAS-X* or *CyO);dinr*^{ex15}*/ TM3Sb,armGFP* males. Parental flies were removed as necessary to prevent overcrowding of progeny. Eclosed non-Sb adult male or female progeny were collected separately by gender in fresh food vials and were individually weighed in an ATI Cahn C-33 microbalance approximately 3 to 18 days after eclosion.

For the R-cell axon guidance rescue analysis, *arm-GAL4/arm-GAL4; FRT82Bdinr*^{273}*/TM6BTb,GFP* virgin females were crossed to *UAS-X/UAS-X; dinr*^{ex15}*/TM6BTb,GFP* males. Parental flies were removed as necessary to prevent overcrowding of progeny. Non-Tubby (Tb) progeny at the wandering third-instar larval or white prepupal stages were dissected, fixed, and stained with MAb24B10 to visualize R-cell axon guidance patterning.

Ilp2^{1} and *Ilp4*^{1} null mutants (Gronke et al., 2010) were obtained from Bloomington Drosophila Stock Center at Indiana University (stock numbers were 30881 and 30883 respectively). *Df[dilp]* flies were generated in our lab by H. Zhang (Zhang et al., 2009). *UAS-dilp* lines for all seven *dilps* were obtained from the lab of E. Hafen.

2.3 Photoreceptor axon guidance analysis

Eye-brain complexes were dissected from third-instar larvae or white prepupae in phosphate-buffered saline (PBS). A protocol obtained from C.H. Lee was used for the staining of eye-brain complexes with monoclonal antibody 24B10 (MAb24B10). MAb24B10 specifically stains the cell bodies and axonal membranes of differentiated photoreceptors in *Drosophila melanogaster* and was originally generated by Fujita et al. (1982). This antibody was subsequently found to recognize the glycoprotein Chaoptin, which resides on the plasma membranes of photoreceptors (Van Vactor et al., 1988). MAb24B10 used in our experiments was purchased from the Developmental Studies Hybridoma Bank at The University of Iowa. The general steps followed were: eye-brain complexes were fixed in 2% paraformaldehyde in a lysine-phosphate buffer containing 0.25% sodium m-periodate, washed in 0.5% Triton-X-100 in PBS (PBT), blocked in 10% normal goat serum (NGS) in PBT, incubated in 1:200 MAb24B10 in 10% NGS in PBT at 4°C overnight or longer, washed in PBT, incubated in 1:200 HRP-conjugated goat anti-mouse antibody in 10% NGS in PBT at room temperature for at least two hours, washed in PBT, incubated in DAB, washed in PBS, and cleared and mounted in 70% glycerol in PBS. Mounting of

the eye-brain complexes involved squashing each with a coverslip in order to obtain flat specimens for imaging with differential interference contrast (DIC) microscopy, using a Leica DMRB microscope. The squashing sometimes led to unfortunate damage to the samples, ranging from artifactual tissue distortion and rips, that nevertheless still allowed the samples to be analyzed, to total destruction of the samples that rendered them unanalyzable.

In an attempt to improve the ease of obtaining analyzable specimens, confocal imaging of eye-brain complexes expressing a red fluorescent protein (RFP) marker in the R-cell axons, under the control of the GMR promoter, was used for the analysis of some *Df[dilp1-5]* mutants. These specimens thus did not have to be stained, and since they could be imaged by confocal microscopy, they did not have to be squashed with coverslips. Confocal imaging was conducted using a Zeiss 510 META laser-scanning microscope, with the kind permission and assistance of C.H. Lee and C.Y. Ting at the National Institutes of Health. Deconvolution of the images using Huygens professional software (Scientific Volume Imaging) and image rendering using Imaris software (Bitplane Inc.) were generously done by C.Y. Ting.

2.4 Allometry analysis

Wings were dissected in 70% ethanol and mounted in 4:5 lactic acid:ethanol. Genital arch posterior lobes were dissected in 70% ethanol, dehydrated in a series of 90% ethanol and 100% ethanol, and mounted in euparol. These slides were placed at ~55°C to allow the euparol to harden. Wings were photographed using a 5× objective, while genital arch posterior lobes were photographed using a 40× objective. The areas

of the wings and genital arch posterior lobes were measured after outlining specific parts of each using the "Polygon selections" tool in ImageJ. (Note: the above was published with slight alterations in Zhang et al. (2009), but was originally written by C. Li)

2.5 Multiple sequence alignment

Insulin receptor sequences for 12 *Drosophila* species which have had their whole genomes sequenced were obtained from Flybase (release r1.2 for *D. virilis*; r1.3 for *D. ananassae*, *D. erecta*, *D. grimshawi*, *D. mojavensis*, *D. persimilis*, *D. sechellia*, *D. simulans*, *D. willistoni*, *D. yakuba*; r2.3 for *D. pseudoobscura*; and r5.16 for *D. melanogaster*). The sequence used for the human insulin receptor was that of the long preproprotein isoform (NCBI reference sequence: NP_000199.2). All of these sequences were aligned together using ClustalW2 at the EMBL-EBI web server; the multiple sequence alignment was then edited using Jalview and Adobe Illustrator.

2.6 Expression level analysis

arm-GAL4/arm-GAL4;FRT82Bdinr^{273}/TM6BTb,GFP virgin females were crossed to males that were homozygous for the following tested Myc-tagged transgenes and lines: *UAS-dinr*, *UAS-dinr(5NPXF)*, *UAS-dinr(JM-NPFF)* line #1, *UAS-dinr(JM-NPFF)* line #2, *UAS-dinr(Y7,8,9,10F)*, and *UAS-dinr(LESL,Y2F)*. For all the tested transgenes and lines, the males also carried the *dinr^{ex15}* allele and the *TM6BTb,GFP* balancer, except for *UAS-dinr(JM-NPFF)* line #2, for which the males

carried the *TM3Sb,armGFP* balancer instead, because a stock carrying the *TM6BTb,GFP* balancer had not been made. Embryos were collected from the crosses, dechorionated in a 1:2 dilution of bleach, and fixed for 15 minutes, with agitation, in a 4% paraformaldehyde in PBS solution that was mixed 1:1 with heptane. The aqueous (lower) phase containing the paraformaldehyde was removed. Methanol was added to the tube and the tube was shaken and vortexed in order to devitellinize the embryos. The heptane (upper) layer was removed along with embryos floating at the interface because they had not devitellinized. The remaining embryos that had devitellinized and had sunk down to the bottom of the methanol (lower) layer were then rinsed two to three times with fresh methanol, and stored in a fresh aliquot of methanol at -20°C.

The following steps for anti-Myc staining and staining level analysis were modified from a protocol developed by J. Hou in the Pick lab. Stored embryos were rehydrated in 0.05% Tween 20 in phosphate-buffered saline (PBST) for 30 minutes, blocked in 5% normal goat serum (NGS) for 30 minutes at room temperature, incubated in 1:1500 preabsorbed anti-Myc antibody (Santa Cruz Biotechnology, Inc. c-Myc (A-14) rabbit polyclonal IgG) overnight at 4°C, rinsed once with PBST, washed twice for 30 minutes each in PBST, incubated in 1:600 Texas Red-X goat anti-rabbit IgG (Invitrogen) for approximately 2.5 hours at room temperature, rinsed once in PBST, washed twice for 30 minutes each in PBST, washed overnight in PBST, rinsed once in PBS, and cleared in 70% glycerol in PBS overnight at 4°C. Fluorescence was detected using the Texas Red filter on a Leica DMRB microscope. Side views of embryos at stages 7 to 11, approximately, were photographed. Adobe

Photoshop was used to quantitate protein expression levels of each overexpressed Myc-tagged DInR construct, as revealed by anti-Myc staining. The same general ventral area of each embryo was selected using the elliptical marquee tool, which was set to a fixed size of 25 pixels width by 25 pixels height, and the mean value for the red channel on the histogram palette (a measure of the average intensity) was recorded and averaged for each DInR transgene.

Chapter 3: Investigating the roles of *dilps* in photoreceptor (R-cell) axon guidance

3.1 Introduction

DInR localized in photoreceptors is required for photoreceptor axon guidance (Song et al., 2003). Since DInR is a receptor tyrosine kinase, it is expected to need an extracellular ligand for activation of all of its downstream signaling functions. In order to more completely understand the mechanism by which insulin receptors direct axon guidance, it is necessary to define the interactions of the insulin receptors and their upstream ligands during this process. However, the ligand(s) that directs the photoreceptor axon guidance function of DInR is unknown.

There are several criteria that, if fulfilled, would provide either definitive or supporting evidence that a candidate molecule is an endogenous ligand for DInR during DInR-mediated photoreceptor axon guidance. These criteria are:

1) loss-of-function mutants of the candidate ligand would exhibit similar defects in photoreceptor axon guidance as have been described for *dinr* mutants,

2) the candidate ligand would be present at the right time and place within or adjacent to the third-instar larval optic lobe, the target site for the R-cell axons,

3) the candidate ligand could bind to and modulate DInR function by activating (or repressing, if the ligand is inhibitory) DInR autophosphorylation,

4) if DInR is dependent on a strict concentration range, or gradient perhaps, of its ligand during photoreceptor axon guidance, then altered levels of the candidate ligand within or adjacent to the third-instar larval optic lobe might lead to defective

axon guidance. Altered levels of the candidate ligand can be achieved experimentally by overexpression. However, failure to see a phenotype caused by overexpression would not necessarily mean that the overexpressed molecule is not a ligand since it is possible that overexpression might not perturb the protein gradient, depending on the gradient-forming mechanism.

5) the candidate ligand would be similar, sequence-wise and/or structurally, to mammalian insulin, since the potential ligand binding domains of DInR and the human insulin receptor share considerable sequence identity (Fernandez et al., 1995).

Based on the available evidence at the beginning of my studies, the most likely candidate ligands for DInR during DInR-mediated photoreceptor axon guidance were the seven *Drosophila* insulin-like peptides (*dilps*), which share sequence similarity with human insulin (Brogiolo et al., 2001). The *dilps* thus fulfill criterion #5 listed above. Also, criterion #3 is fulfilled for some of the DILPs because Rulifson *et al.* (2002 and unpublished work) showed using cell culture that some of the DILP proteins can activate DInR autophosphorylation.

Gain-of-function (GOF) approaches to the study of genes can provide evidence that complements loss-of-function (LOF) studies. In some cases, GOF approaches can even yield insights where LOF approaches fail. Examples of such cases are: 1) the LOF phenotype is not readily assayable, 2) genetic redundancy prevents or partially obscures the manifestation of a LOF phenotype, 3) if a gene is pleiotropic, then a defect in one process (e.g. cell proliferation) may prevent or complicate the analysis of a possible defect in another process (reviewed in Miklos and Rubin, 1996). The last two examples might apply for the study of *dilp* function in

photoreceptor axon guidance, since there are multiple candidate ligands for DInR, a receptor known to have multiple functions.

The GAL4 system is commonly used in *Drosophila* research to overexpress candidate genes in a temporally and spatially-specific manner. Crosses are done to generate flies that carry both of the following transgenes: 1) a transgene that allows the yeast transcriptional activator GAL4 to be expressed under the control of a specific *Drosophila* enhancer sequence, 2) a transgene that contains both an upstream activation sequence (UAS), which consists of GAL4 binding sites, and the gene of interest. The flies will therefore overexpress the gene of interest in the pattern dictated by the specific enhancer sequence (Brand and Perrimon, 1993). Some GOF studies of *dilps* have already been done by others. Each of the seven *dilp* genes has been reported to cause overgrowth when overexpressed (Ikeya et al., 2002). These results were obtained using the ubiquitous driver *arm-GAL4* to drive expression of *UAS* transgenes for each *dilp*. Interestingly, when *Act5C-GAL4*, another ubiquitous driver that is thought to drive stronger expression than *arm-GAL4*, was used to overexpress *dilp2*, lethality resulted during the embryonic stage (Brogiolo et al., 2001).

Loss-of-function (LOF) studies provide the most definitive genetic evidence that a gene is involved in a particular process. However, only suggestive evidence is provided for a gene not being involved in a process because genetic redundancy might prevent the appearance of a LOF phenotype. Since it was hypothesized that one or several of the seven *dilps* are involved in photoreceptor axon guidance by acting as ligands for DInR, the seven *dilps* were removed individually or in combination by different approaches. The removal of individual *dilp* genes would allow the

determination of whether one specific *dilp* gene is required for photoreceptor axon guidance. The removal of multiple *dilp* genes would allow the determination of whether several *dilp* genes are involved redundantly in photoreceptor axon guidance.

3.2 Results: gain-of-function studies

In order to determine whether ubiquitous overexpression of any of the *dilps* leads to a GOF phenotype, MAb24B10-stained eye-brain complexes from third-instar larvae containing either a *da-GAL4* transgene, which drives strong ubiquitous expression, or an *arm-GAL4* transgene, which drives moderate ubiquitous expression, and one *UAS-dilp*"*x"* transgene (one fly line for each of the seven *dilps* was obtained from E. Hafen) were examined for defects in photoreceptor axon guidance. Controls contained the *da-GAL4* transgene only or the *arm-GAL4* transgene only. Photoreceptor axon guidance in these controls (Figure 5A,C) resembled that of WT (Figure 10B). Thus, the presence of the *da-GAL4* transgene itself or the *arm-GAL4* transgene itself did not cause axon guidance defects. Third-instar larvae in which *da-GAL4* drove the *UAS-dilp2* transgene (*daGAL4>UAS-dilp2*) were not viable, so the R-cell axon guidance phenotype was not assessed. The effect of overexpression of *dilp7* was not studied. Ubiquitous overexpression of *dilp1, dilp3*, *dilp5*, or *dilp6* did not cause any obvious photoreceptor axon guidance phenotypes (Figure 5E-H), although occasionally, overexpression of *dilp1* gave a phenotype somewhat resembling the phenotype from overexpression of *dilp4* (described below).

The ubiquitous overexpression of *dilp4* led to a mild photoreceptor axon phenotype. When overexpressed by the strong *da-GAL4* driver, growth cones in the medulla appeared unusually distinct (Figure 5B; yellow arrowhead) and there seemed

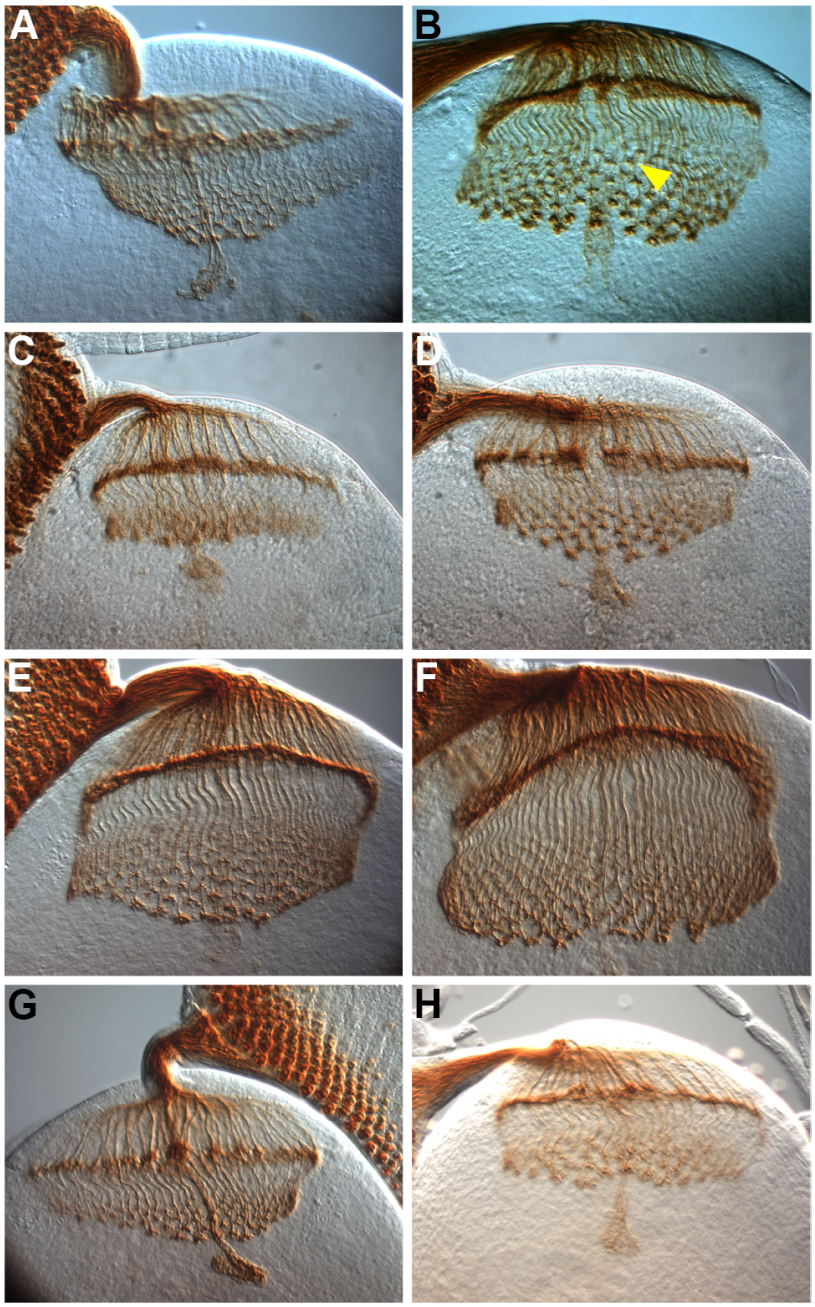
A
B
C
D
E
F
G
H

Figure 5. Ubiquitous overexpression of *dilp4* led to a gain-of-function phenotype. Third-instar larval eye-brain complexes were stained with MAb24B10. (A) *da-GAL4*, by itself, served as the negative control for specimens shown in panels (B) and (E-H). (B) *dilp4* was ubiquitously overexpressed by the strong *da-GAL4* driver (*da-GAL4>UAS-dilp4)*. (C) *arm-GAL4*, by itself, served as the negative control for the specimen in panel (D). (D) *dilp4* was ubiquitously overexpressed by the moderate *arm-GAL4* driver. (E) *da-GAL4>UAS-dilp1*. (F) *da-GAL4>UAS-dilp5*. (G) *da-GAL4> UAS-dilp6*. (H) *da-GAL4>UAS-dilp3*. The yellow arrowhead in B points to an example of a growth cone in the medulla that appears to be unusually pronounced in appearance.

to be an increased distance between the growth cones (Figure 5B) as compared to the control (Figure 5A). Quantitation of the distance between the growth cones was not done because the squashing of the specimens for DIC imaging meant that quantitation would be inaccurate if different specimens were flattened more than others. However, the growth cone characteristics were recognizable in blind experiments. In a sense, the gain-of-function growth cone phenotype is the opposite of the *dinr* loss-of-function phenotype which consists of clumped axons and unexpanded growth cones (Song et al., 2003). When *dilp4* was ubiquitously overexpressed by the moderate *arm-GAL4* driver, a similar but weaker phenotype was observed (Figure 5D) that was distinguishable from the control (Figure 5C). However, the mild overexpression phenotypes seen for *dilp4* were not seen for every specimen.

3.3 Results: loss-of-function studies

Since the overexpression of *dilp4* led to a subtle phenotype, photoreceptor axon guidance was examined in animals in which *dilp4* was knocked down by RNAi. Two different *UAS-dilp4 RNAi* lines made by H. Zhang using the pWIZ RNAi vector (Lee and Carthew, 2003) were expressed ubiquitously using the *da-GAL4* driver. Photoreceptor axon guidance appeared essentially normal (Figure 6A,B). The reduction of *dilp1, -2, -3,* and *-5* levels together was achieved by ablating cells that express these *dilps* by using *dilp2-GAL4* to drive the expression of the proapoptotic gene *reaper.* This did not appear to have an effect on photoreceptor axon guidance (Figure 7B). Various genetic deficiencies that uncover *dilp* genes were also

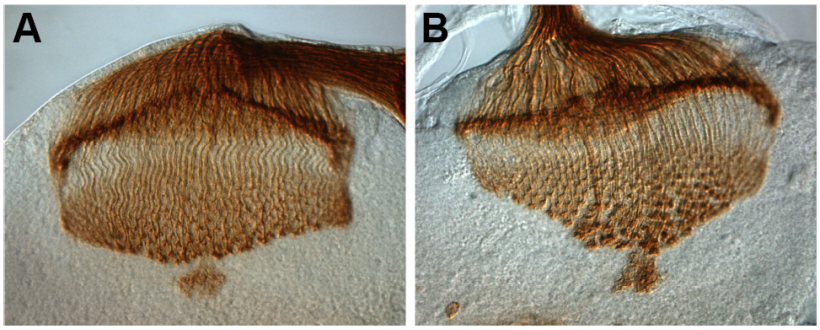

Figure 6. RNAi against *dilp4* did not affect photoreceptor axon guidance. Eye-brain complexes from prepupae were stained with MAb24B10. (A) *da-GAL4>UAS-dilp4 RNAi* line #1. (B) *da-GAL4> UAS-dilp4 RNAi* line #2.

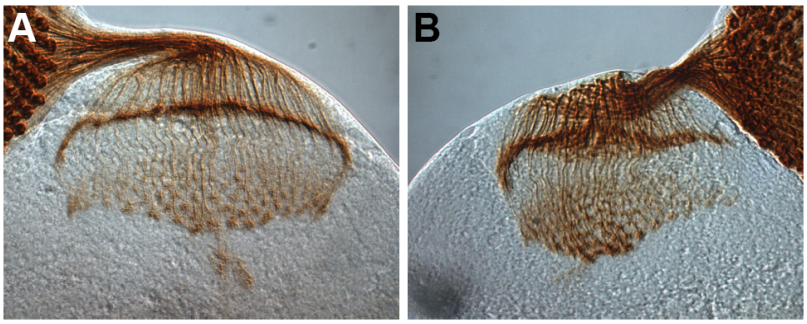

Figure 7. Reduction of *dilp1*, *-2*, *-3*, and *-5* levels did not perturb photoreceptor axon guidance. Eye-brain complexes from third-instar larvae were stained with MAb24B10. (A) Negative control eye-brain complex from a larva carrying the *dilp2-GAL4* driver only. (B) Eye-brain complex from a larva in which the *dilp1, -2, -3,* and *-5*-expressing cells were ablated by expressing the propapoptotic gene *reaper* using the *dilp2-GAL4* driver.

generated, using a FLP-FRT-based method (Parks et al., 2004), by H. Zhang. *Df[dilp1-5]* uncovers *dilp1*, *-2*, *-3*, *-4*, *-5*, and four flanking genes on the third chromosome, due to the locations of the FRT sites used to generate the deficiency (Zhang et al., 2009). To determine whether *dilps 1-5* regulate photoreceptor axon guidance, eye-brain complexes from *Df[dilp1-5]* third-instar larvae, which are smaller than wild type controls (Zhang et al., 2009) and thus more challenging to dissect, were examined by staining with MAb24B10 and imaging with DIC optics, or by expressing RFP in the photoreceptor axons and imaging with confocal microscopy. A total of seven *Df[dilp1-5]* specimens were analyzed. The sole analyzable *Df[dilp1-5]* specimen that was stained with MAb24B10 (Figure 8B) appeared normal when compared to the w^{1118} control (Figure 8A). In order to obtain more analyzable specimens for *Df[dilp1-5]*, a stock was made in which these mutants express the RFP marker in photoreceptor axons under the control of the GMR promoter. Another six specimens were examined by this method; one specimen is shown in Figure 8H. Part of the larval visual system, the Bolwig's organ, appeared to express RFP at very high levels, but photoreceptor axon guidance in the developing adult visual system appeared normal.

Df[dilp6], made by H. Zhang, uncovers *dilp6* and four flanking genes on the X chromosome (Zhang et al., 2009). No axon guidance defects were seen in the *Df[dilp6]* samples (Figure 8C; n=7). *Df[dilp7]*, also made by H. Zhang, uncovers *dilp7* and two flanking genes on the X chromosome (Zhang et al., 2009). Although axon guidance did not appear completely normal in the *Df[dilp7]* samples (Figure

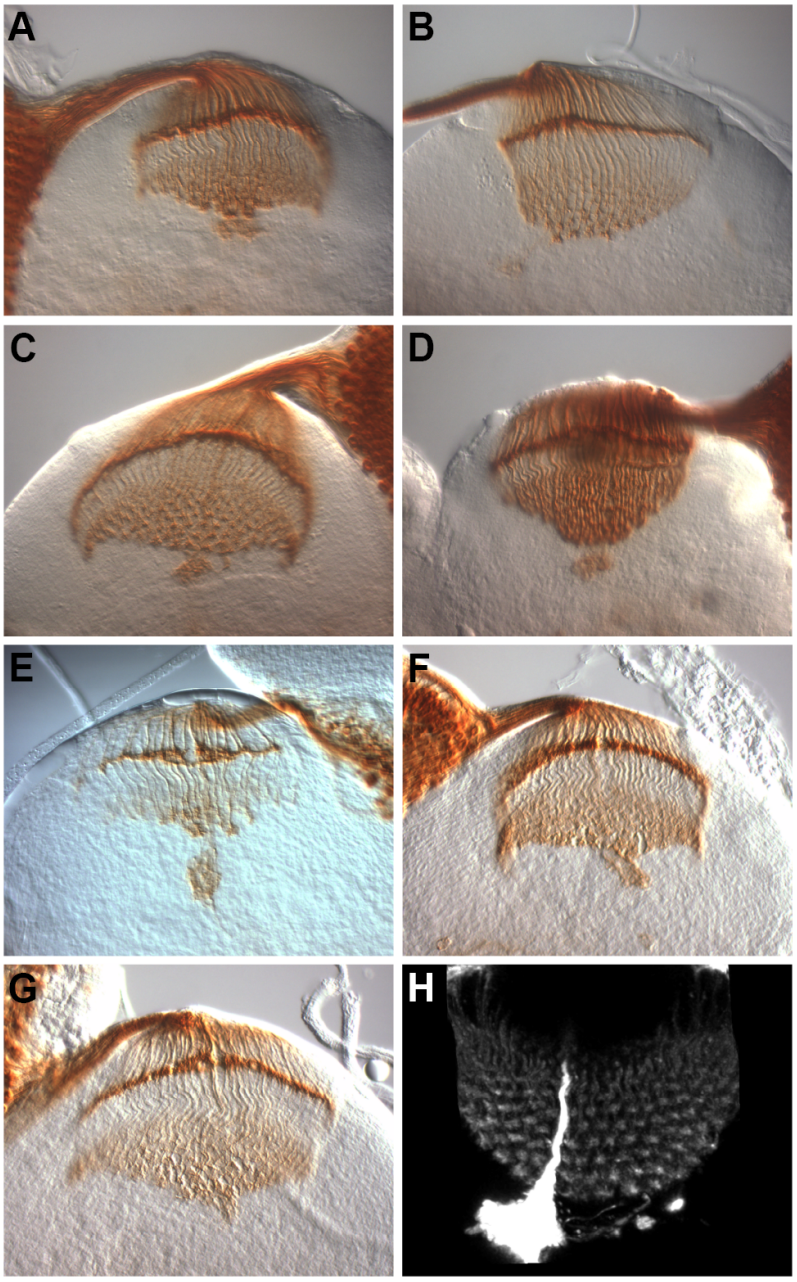
A
B
C
D
E
F
G
H

Figure 8. Loss of individual or combinations of *dilp* genes did not severely disrupt R-cell axon guidance. MAb24B10-stained eye-brain complexes from (A) w^{1118} control, (B) *Df[dilp1-5]*, (C) *Df[dilp6]*, (D) *Df[dilp7]*, (E) *Df[dilp6],Df[dilp7]/Y*, (F) $dilp2^{1}$, and (G) $dilp4^{1}$ third-instar larvae were imaged with DIC optics. (H) shows an eye-brain complex from a *Df[dilp1-5]* animal expressing RFP in photoreceptor axons under the control of the GMR promoter; confocal microscopy was used for imaging. Photos may have been cropped to different magnifications.

8D; n=3), because the growth cones in the medulla seemed to be closer together than normal, it did not resemble the disrupted phenotype of *dinr* mutants.

To determine whether *dilp6* and *dilp7* act redundantly to regulate photoreceptor axon guidance, eye-brain complexes from *Df[dilp6],Df[dilp7]/Y* (*Y* represents the Y chromosome; *dilp6* and *dilp7* are on the X chromosome) hemizygous third-instar larvae were examined. Only one analyzable *Df[dilp6],Df[dilp7]/Y* sample was obtained (Figure 8E). Axon guidance appeared essentially normal in this specimen, although there is a gap present in the lamina which may or may not be an artifact of the mounting procedure. More specimens would have to be examined in order to conclude that photoreceptor axon guidance is relatively normal in the *Df[dilp6],Df[dilp7]/Y* mutant.

Various single and combination mutants of the *dilp* genes generated by homologous recombination (Gronke et al., 2010) recently became available. The $dilp4^{1}$ mutant was obtained and examined since the overexpression of *dilp4* had yielded a mild overexpression phenotype. Photoreceptor axon guidance appeared essentially normal (Figure 8G). The photoreceptor axon guidance in the $dilp2^{1}$ mutant also appeared essentially normal (Figure 8F).

3.4 Discussion

The ligand that directs the photoreceptor axon guidance function of the *Drosophila* insulin receptor is still unknown. My efforts to identify this ligand involved conducting gain-of-function and loss-of-function genetic experiments to test the most likely candidates, the *dilp* genes. The surprising finding from these

experiments was that none of the seven *dilps*, in the combinations examined, seem to be required for R-cell axon guidance. Although a subtle phenotype, involving growth cones that seemed to be unusually distinct and spaced further apart in the medulla, was seen when *dilp4* was overexpressed, the *dilp4* null mutant appeared to have normal photoreceptor axon guidance. *Df[dilp1-5]*, *Df[dilp6]*, *Df[dilp7]*, and *Df[dilp6]*,*Df[dilp7]*/*Y* mutants also lacked the severe photoreceptor axon guidance defects seen in *dinr* mutant transheterozygotes. A mutant for the ligand(s) of DInR would be expected to give a phenotype of similar severity to *dinr* mutants. However, it is still possible that genetic redundancy underlies the lack of a strong phenotype seen in the mutants examined so far, since only *dilp1-5*, and *dilp6-7* were removed in combination. If this were to be further pursued, I would suggest that a triple *dilp1;dilp4;dilp7* mutant be examined, as these were the three genes that showed some suggestion of function in the assays I have done. Interestingly, Gronke et al. (2010) recently generated and examined different combinations of *dilp* mutants and found evidence suggesting that *dilp1*, *dilp4*, and *dilp7* are not involved in regulating developmental timing. Furthermore, since I have obtained evidence indicating that photoreceptor axon guidance is not affected by developmental delay (Chapter 5 of this thesis), this supports the appealing hypothesis that developmental timing and photoreceptor axon guidance are controlled by different *dilps.* Further evidence obtained by Gronke et al. (2010) supporting the involvement of DILP4 in photoreceptor axon guidance was the observation of DILP4 antibody staining in neurons throughout the brain. To our knowledge, no one has tested whether DILP1 or DILP7 protein is present in the brain.

A second possibility is that none of the seven *dilps* regulate R-cell axon guidance; instead another molecule might be the actual ligand. A third formal possibility is that no ligand is actually required for DInR to direct photoreceptor axon guidance, so that the mere presence of DInR is permissive for normal axon guidance to occur. However, this possibility is unlikely since Song et al. (2003) showed that autophosphorylation of DInR is required for DInR and Dock binding, and it is known that autophosphorylation of DInR depends upon ligand-binding (Saltiel and Kahn, 2001). To further confirm the requirement for ligand-binding by DInR in photoreceptor axon guidance regulation, the extracellular ligand-binding region of DInR could be removed and the resulting construct could be tested to see whether it can rescue the photoreceptor axon guidance defects of *dinr* mutants.

To test the possibility that another molecule might act as the DInR ligand during photoreceptor axon guidance, one could try using a biochemical approach to purify the ligand from third-instar larval extracts. The ability of various fractions to activate DInR autophosphorylation could be used as an assay during the purification process. Once the candidate ligands have been isolated, mass spectrometry would be used to identify what they are. If the molecules are proteins, then genetic mutants deficient for these molecules could be generated and examined for photoreceptor axon guidance defects. Alternatively, a genetic screen could be carried out to identify genes encoding putative ligands.

Chapter 4: Involvement of *dilps* in allometry

Note: this work was published in Zhang et al. (2009) as Figure 3.

4.1 Introduction

Allometry is a term that refers to the scaling of the size of different body parts relative to each other or to the entire body size (reviewed in Shingleton et al., 2007). Shingleton et al. (2005) implicated insulin signaling in the regulation of allometry in *Drosophila*. In the *dinr* transheterozygotes that they studied, the wings and maxillary palps scaled down in proportion to overall body size, but the genital arch posterior lobes did not. They saw similar results with *chico* mutant clones. Thus, they interpreted their results to mean that particular organs, such as the genitals, are less affected by changes in insulin signaling.

H. Zhang used a FLP-FRT-based method (Parks et al., 2004) to generate a mutant, *Df[dilp1-5]*, that uncovers *dilp1*, *-2*, *-3*, *-4*, *-5*, and four flanking genes on the third chromosome (Zhang et al. 2009). In order to determine whether *dilps 1-5* are involved in controlling allometry, I dissected wings and genital arch posterior lobes from parental controls and *Df[dilp1-5]* homozygotes and measured the area of each.

4.2 Results

The wings of the *Df[dilp1-5]* homozygotes were approximately 29% smaller than those of the parental controls (Figure 9). In contrast, the genital arch posterior lobes of the *Df[dilp1-5]* homozygotes were only approximately 15% smaller than those of the parental controls. These numbers are consistent with those published by

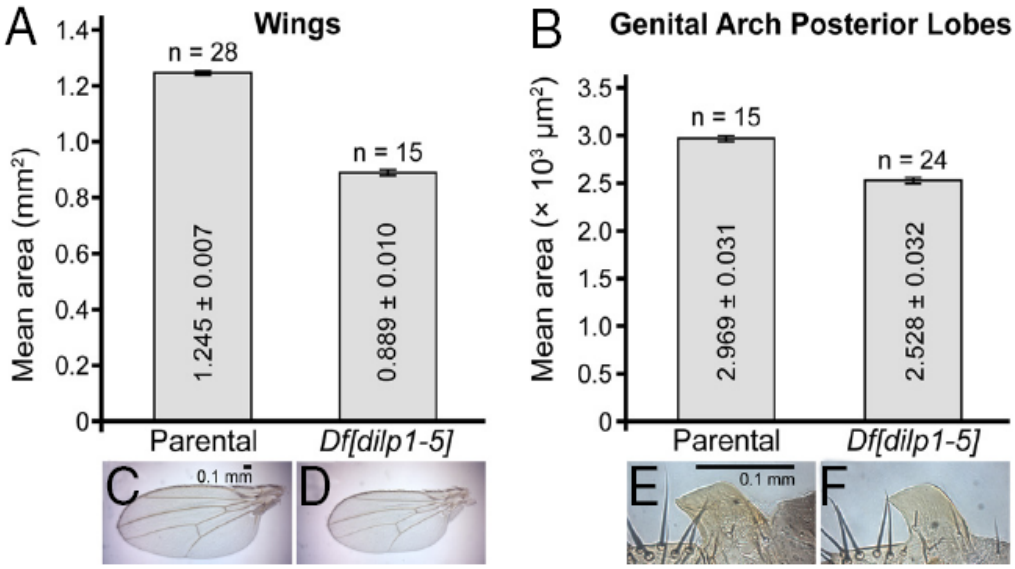

Figure 9. *dilp1, -2, -3, -4,* and/or *-5* are required for allometry in *Drosophila*. (A) Mean areas of wings from parental controls (line d02657, which was used to generate *Df[dilp1-5]*) and *Df[dilp1-5]* homozygotes. *Df[dilp1-5]* wings are approximately 29% smaller than control wings. (B) Mean areas of genital arch posterior lobes from parental controls and *Df[dilp1-5]* homozygotes. *Df[dilp1-5]* genital arch posterior lobes are only approximately 15% smaller than those of controls. (C) A representative parental control wing. (D) A representative *Df[dilp1-5]* wing. (E) A representative parental control genital arch posterior lobe. (F) A representative *Df[dilp1-5]* genital arch posterior lobe. Error bars represent standard errors.

Shingleton et al. (2005) and indicate that the size of the male genitals are not as affected by the loss of *dilps 1-5* as the wings.

4.3 Discussion

This experiment shows that *dilp1, -2, -3, -4,* and/or *-5* are involved in the establishment of allometry, and thus might be the ligand(s) to activate DInR and recruit the Chico downstream signaling pathway in this process. It is possible, however, that only a subset of the 5 *dilps* tested in combination are actually involved in allometry control. Thus, future experiments could examine allometry in single *dilp* mutants and in mutants containing smaller combinations of *dilp* mutations. Also, genetic interaction or epistasis experiments could be done to confirm that the implicated *dilp*(*s*) does act through DInR and Chico to control allometry.

Chapter 5: Developmental delay does not underlie the axon guidance defects in *dinr* mutants

5.1 Introduction

The *Drosophila* insulin receptor (DInR) is essential for proper photoreceptor axon guidance (Song et al., 2003). For instance, photoreceptor axons in $dinr^{353/273}$ transheterozygotes are disorganized, showing clumps and gaps in their targeting pattern. However, the pleiotropic functions of DInR, such as in cell growth (Chen et al., 1996), complicate the study of the role of DInR in specific tissues or cell types. Although two lines of evidence using different approaches – that is, *dinr* mutant mosaic analysis and transheterozygote analysis – indicated that DInR is involved in regulating photoreceptor axon guidance (Song et al., 2003), each approach has advantages and disadvantages regarding interpretation of the results that were generated for the *dinr* mutants. A problem with mosaic analysis is that the size of the photoreceptor cells in *dinr* mutant eye clones is smaller than normal. The axons of these small mutant cells innervate a target composed of normal sized cells. Therefore, the axon guidance defects in the mosaic animals may be a secondary effect of a mismatch in sizes of the mutant photoreceptor axons and the target cells. This problem is avoided when *dinr* mutant transheterozygotes are analyzed. Since the whole animal is mutant in the transheterozygotes, all cells are presumed to be equally reduced in size. However, *dinr* mutant transheterozygote analysis presents its own challenges. Since *dinr* mutant transheterozygotes are developmentally delayed, the

photoreceptor axon guidance defect may be a secondary result of the developmental delay.

In order to determine whether developmental delay contributes to the photoreceptor axon guidance defects in the *dinr* mutant transheterozygotes, third-instar larvae at different stages of development and prepupae were stained with MAb24B10 (Fujita et al., 1982) to visualize differentiated photoreceptors and their axons. An approximation of the developmental stage of each third-instar larva was obtained by estimating the number of rows of differentiated photoreceptors in the eye disc. Specimens were placed in three classes: 1) approximately 5-10 rows, 2) more than approximately 10 rows, and 3) prepupae.

If the photoreceptor axon guidance phenotypes of the "early stage" (i.e. in the ~5-10 rows class) WT and control eye-brain complexes resembled the phenotype of the "late stage" (i.e. in the >~10 rows class or prepupae) *dinr* mutant transheterozygotes, with axonal clumping and gaps in the axonal targeting pattern, then this would indicate that developmental delay does indeed contribute to the axon guidance defects of *dinr* mutant transheterozygotes. The potential impact of developmental delay would thus have to be taken into account in future experiments. However, if the "early stage" WT and control eye-brain complexes did not resemble the phenotype of the "late stage" *dinr* mutant transheterozygotes, then this would show that developmental delay does not impact proper axon guidance.

5.2 Results

Developmental time courses of photoreceptor axon guidance were analyzed in

eye-brain complexes isolated from OreR, w^{1118}, and ry^{506} third-instar larvae and prepupae. OreR was chosen for the analysis because it is a wild type strain, ry^{506} because the $dinr^{ex15}$ null allele was generated in a *ry* background (Song et al., 2003), and w^{1118} because it is the background for the *UAS-dilp* transgenic flies used for the *dilp* overexpression studies (Brogiolo et al., 2001; Ikeya et al., 2002). The eye-brain complexes were stained with MAb24B10 (Fujita et al., 1982) to visualize the differentiated photoreceptors and their axons. In order to provide an approximation of the developmental stages of the eye-brain complexes from third-instar larvae, the numbers of rows of differentiated photoreceptors in the eye discs were estimated. Based on this number, specimens were placed in these classes for analysis: ~5-10 rows and more than ~10 rows. For the w^{1118} and ry^{506} genotypes, eye-brain complexes from prepupae were also analyzed.

As expected, OreR eye-brain complexes at a later stage of development, with >~10 rows of differentiated photoreceptors, showed targeting of axons to the lamina that resulted in a relatively thin, continuous layer of axon terminals (arrow in Figure 10B) and targeting of other axons to the medulla that resulted in a wide pattern of staggered growth cones (bracket in Figure 10B)(n=3). Notably, OreR complexes at an earlier stage of development, with ~5-10 rows, also showed similar patterns of axonal targeting to the lamina and the medulla (Figure 10A; n=6).

Eye-brain complexes from ry^{506} and w^{1118} animals also displayed ordered targeting of axons to the lamina and medulla, regardless of whether the complexes

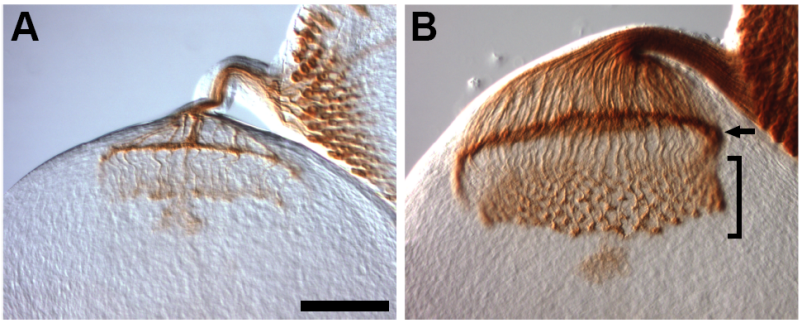

Figure 10. Developmental time course of R-cell axon guidance in OreR third-instar larvae. The complex in (A) is at the ~5-10 rows stage, containing approximately 6 rows of differentiated photoreceptors. The complex in (B) is at the >~10 rows stage, containing approximately 12 rows. The arrow in (B) points to axons terminating in the lamina to form a thin, continuous layer. The bracket in (B) indicates axons terminating in the medulla to form a staggered array of growth cones. The complexes were stained with MAb24B10 and were imaged using a 40× objective and DIC optics. The scale bar represents approximately 50 μm.

were at the ~5-10 rows stage (ry^{506}, n=17, Figure 11A; w^{1118}, n=10, Figure 12A), at the >~10 rows stage (ry^{506}, n=14, Figure 11B; w^{1118}, n=28, Figure 12B), or from prepupae (ry^{506}, n=1, Figure 11C; w^{1118}, n=3, Figure 12C). Occasionally, there were small clumps seen in ry^{506} eye-brain complexes (2/17 at the ~5-10 rows stage, see arrow in Figure 11D; 1/14 at the >~10 rows stage). Expanded growth cones in the medulla were present during all stages (an example is shown with an arrow in Figure 11E). In some complexes that were analyzed, gaps in the lamina were present which may or may not have been artifacts of the mounting procedure (arrow in Figure 11B).

Overall, the ordered targeting pattern of photoreceptor axons to the lamina and medulla at early stages of axon guidance in the wild type (OreR) and control (w^{1118} and ry^{506}) larvae does not resemble the disorganized targeting pattern of axons at later stages of axon guidance in the *dinr* mutant transheterozygotes (Song et al., 2003). These results indicate that the axon guidance phenotype exhibited by the *dinr* mutant transheterozygotes is not merely due to axon guidance proceeding at a slower pace than usual.

Perhaps also of interest are the expanded medullar growth cones that were observed in early-stage control eye-brain complexes. It is difficult to say with certainty whether there are inappropriately unexpanded growth cones actually present in *dinr* mutant transheterozygotes since the disorganized axonal targeting can obscure the gradient of young to old growth cones normally present in the medulla (Ting and Lee, 2007). Furthermore, in *dinr* mutant transheterozygotes, it is hard to determine whether the growth cones of axons in the clumps are expanded or unexpanded. Although abnormally unexpanded growth cones have been observed in *dinr* mutant

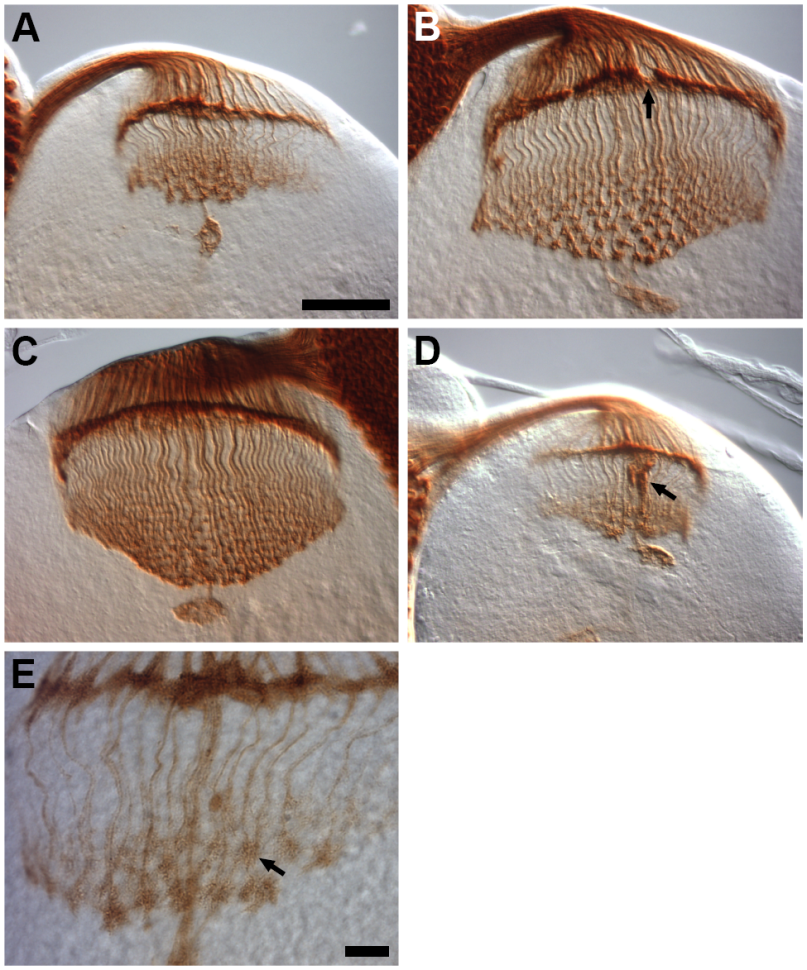

Figure 11. Developmental time course of R-cell axon guidance in *ry*^{506} animals. The complexes in (A), (D), and (E) are at the ~5-10 rows stage, (B) is at the >~10 rows stage, and (C) is from a prepupa. The approximate numbers of rows of differentiated photoreceptors for the complexes from third-instar larvae were: (A) 8, (B) 13, (D) 8, and (E) 6. The arrow in (B) points to a gap in the lamina. Occasionally,

there were abnormal clumps present in the ry^{506} complexes (arrow in D). Expanded growth cones were present at all stages, even at the ~5-10 rows stage. The arrow in (E) points to an expanded growth cone in a complex at the ~5-10 rows stage seen at higher magnification. The complexes were stained with MAb24B10 and were imaged using a 40× objective and DIC optics for (A-D) and a 100× oil immersion objective and bright field optics for (E). The scale bar for (A-D) indicates approximately 50 μm. The scale bar for (E) represents approximately 10 μm.

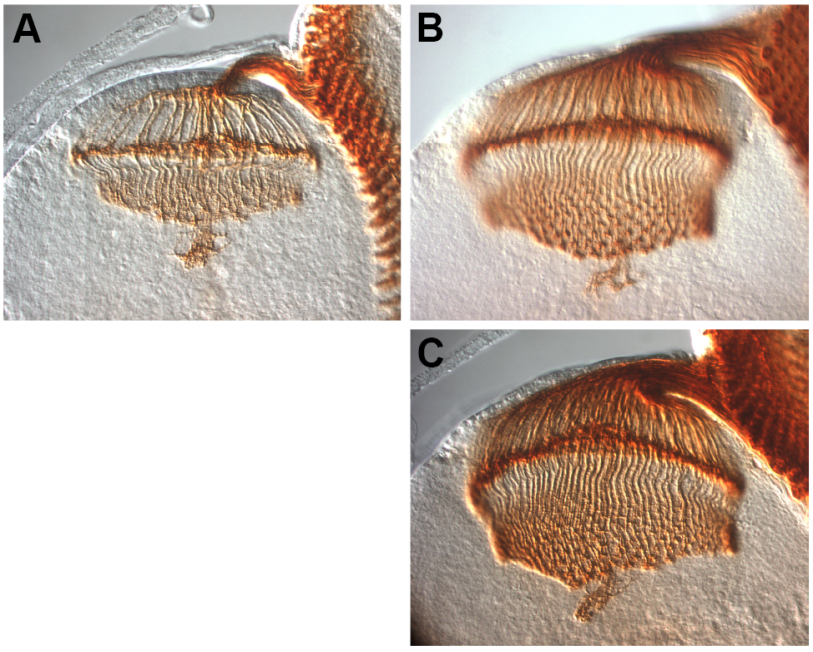

Figure 12. Developmental time course of R-cell axon guidance in *w*^{1118} animals. The complex in (A) is at the ~5-10 rows stage, containing approximately 7 rows of differentiated photoreceptors. The complex in (B) is at the >~10 rows stage, containing approximately 15 rows. The complex in (C) is from a prepupa. The complexes were stained with MAb24B10 and were imaged using a 40× objective and DIC optics.

clones (Song et al., 2003), the developmental time course of axon guidance in control animals presented here does not directly apply to the analysis of *dinr* mutant clones; the appropriate controls for the *dinr* clonal analysis were WT clones, which were indeed generated and analyzed by Song et al. (2003).

5.3 Summary

These results indicate that developmental delay is not a significant factor underlying the R-cell axon guidance defects seen in *dinr* mutant transheterozygotes (Song et al., 2003) since the R-cell axon guidance phenotype of "early stage" control eye-brain complexes did not resemble that of "late stage" *dinr* mutant transheterozygotes which are developmentally delayed. Thus it appears that DInR controls photoreceptor axon guidance through a mechanism(s) that is insulated from the whole organism effects of DInR in developmental timing (shown here) and in growth (i.e. *chico* growth mutants lack photoreceptor axon guidance defects (Song et al., 2009)).

Chapter 6: Functional dissection of the signaling domains of the *Drosophila* insulin receptor

6.1 Introduction

The implication of DInR in axon guidance added a novel role for a receptor already known to be involved in regulating diverse developmental and physiological processes such as viability (Fernandez et al., 1995), growth (Chen et al., 1996; Fernandez et al., 1995), and sugar homeostasis (Belgacem and Martin, 2006). This raised the question of how one receptor can control such diverse functions. One strategy is that different downstream pathways are used by DInR to control its different functions. DInR is thought to control growth by interacting with the Chico adaptor protein, which is the *Drosophila* homolog of the mammalian IRS proteins (Bohni et al., 1999). Chico recruits the PI3K-Akt pathway in order to control growth. Adult *chico* mutant homozygotes are much smaller than wild type flies and *chico* mutant heterozygotes. Conversely, DInR controls photoreceptor axon guidance by interacting with the Dock adaptor protein, which is the *Drosophila* homolog of mammalian Nck and which recruits the Pak signaling pathway (Hing et al., 1999). In mammals, Nck is recruited by IRS1 to the insulin receptor (Lee et al., 1993; reviewed in Pawson and Scott, 1997).

Adaptor proteins are composed solely of interaction domains (reviewed in Howard et al., 2003). Examination of the domains that are present in an adaptor protein can provide clues about which motifs an adaptor protein may bind to. Chico has a phosphotyrosine binding (PTB) domain (Poltilove et al., 2000); PTB domains

are known to bind to NPXpY motifs, when the tyrosine is phosphorylated (Pawson and Scott, 1997). Dock has three SH3 domains and one SH2 domain (Garrity et al., 1996). Both the SH3 domains and SH2 domain of Dock were shown by yeast two-hybrid to be required for maximal binding between DInR and Dock (Song et al., 2003). Rao and Zipursky (1998) tested constructs with different point mutations in the SH2 and SH3 domains of Dock and found that mutations in the second SH3 domain alone, or in the first and third SH3 domains and the SH2 domain together, failed to rescue the photoreceptor axon guidance defects of *dock* null mutants. It was also found that Dock binds to its downstream effector Pak through the second SH3 domain (Hing et al., 1999). Taken together with the results of Song et al. (2003), this suggests that the first and third SH3 domains and the SH2 domain might be the domains that bind the upstream receptor DInR to mediate photoreceptor axon guidance. It is known that SH3 domains bind to PXXP motifs, whereas SH2 domains bind to pYXXhy motifs (Pawson and Scott, 1997).

The C-tail of DInR has multiple potential binding motifs. Thus, while many of the protein-protein interactions of mammalian IR require intermediary adaptor proteins, DInR may bind directly. The clearest example of direct signaling through the C-tail came from Song et al. (2003) who showed that Dock directly interacts with the C-tail of DInR in yeast two-hybrid assays. The C-tail contains ten tyrosines, four of which are located within NPXpY motifs (Figure 13A). In addition, it contains three PXXP motifs (Figure 13A). Poltilove et al. (2000) showed that the four NPXpY motifs are important for binding between Chico and DInR in vitro. They tested a deletion of all four NPXpY motifs, but not individual motifs or smaller combinations

A

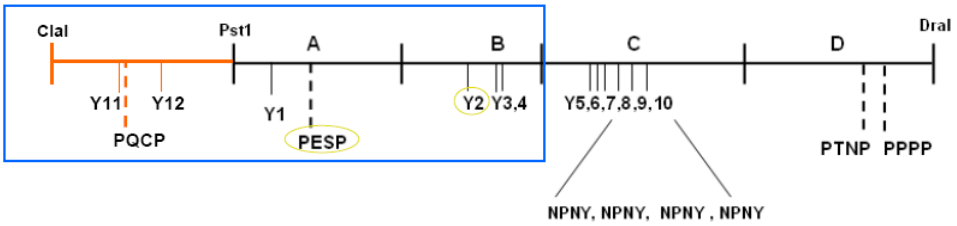
ClaI
Pst1
A
B
C
D
DraI
Y11
Y12
Y1
Y2
Y3,4
Y5,6,7,8,9,10
PQCP
PESP
PTNP
PPPP
NPNY, NPNY, NPNY , NPNY

B

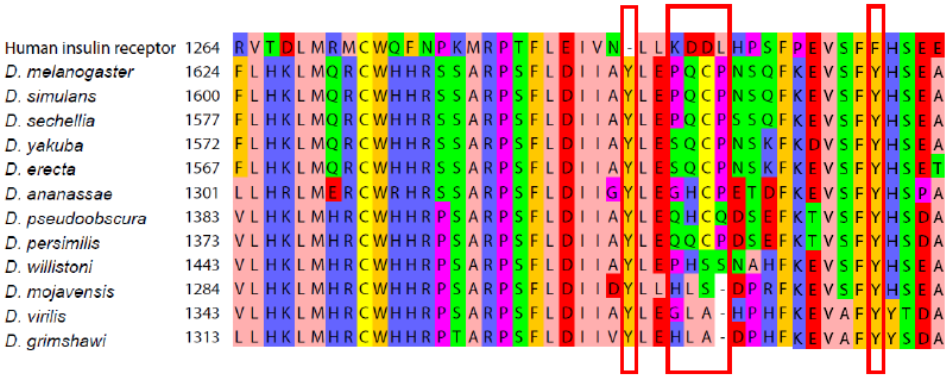
Human insulin receptor 1264 RVTDLMRMCWQFNPKMRPTFLEIVN-LLKDDLHPSFPEVSFFHSEE
D. melanogaster 1624 FLHKLMQRCWHHRSSARPSFLDIIAYLEPQCPNSQFKEVSFYHSEA
D. simulans 1600 FLHKLMQRCWHHRSSARPSFLDIIAYLEPQCPNSQFKEVSFYHSEA
D. sechellia 1577 FLHKLMQRCWHHRSSARPSFLDIIAYLEPQCPSSQFKEVSFYHSEA
D. yakuba 1572 FLHKLMQRCWHHRSSARPSFLDIIAYLESQCPNSKFKDVSFYHSEA
D. erecta 1567 FLHKLMQRCWHHRSSARPSFLDIIAYLESQCPNSKFKEVSFYHSET
D. ananassae 1301 LLHRLMERCWRHRSSARPSFLDIIGYLEGHCPETDFKEVSFYHSPA
D. pseudoobscura 1383 VLHKLMHRCWHHRPSARPSFLDIIAYLEQHCQDSEFKTVSFYHSDA
D. persimilis 1373 VLHKLMHRCWHHRPSARPSFLDIIAYLEQQCPDSEFKTVSFYHSDA
D. willistoni 1443 VLHKLMHRCWHHRPSARPSFLDIIAYLEPHSSNAHFKEVSFYHSEA
D. mojavensis 1284 VLHKLMHRCWHHRPSARPSFLDIIDYLLHLS-DPRFKEVSFYHSEA
D. virilis 1343 VLHKLMHRCWHHRPSARPSFLDIIAYLEGLA-HPHFKEVAFYYTDA
D. grimshawi 1313 LLHKLMHRCWHHRPTARPSFLDIIVYLEHLA-DPHFKEVAFYYSDA

C

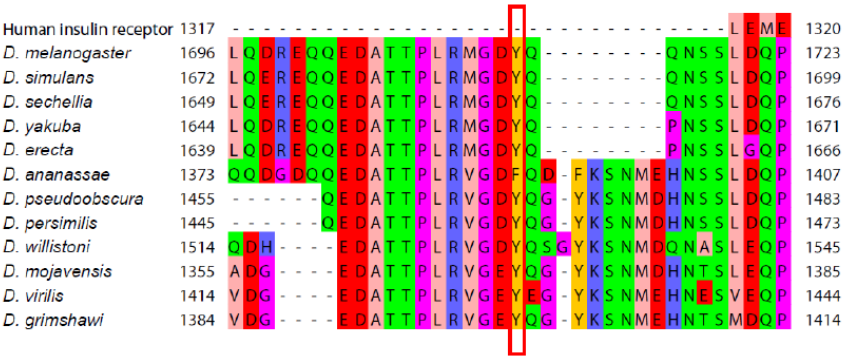
Human insulin receptor 1317 ----------LEME 1320
D. melanogaster 1696 LQDREQQEDATTPLRMGDYQ--------QNSSLDQP 1723
D. simulans 1672 LQERERQQEDATTPLRMGDYQ--------QNSSLDQP 1699
D. sechellia 1649 LQERERQQEDATTPLRMGDYQ--------QNSSLDQP 1676
D. yakuba 1644 LQDREQQEDATTPLRMGDYQ--------PNSSLDQP 1671
D. erecta 1639 LQDREQQEDATTPLRMGDYQ--------PNSSLGQP 1666
D. ananassae 1373 QQDGDQQEDATTPLRVGDFQD-FKSNMEHNSSLDQP 1407
D. pseudoobscura 1455 ------QEDATTPLRVGDYQG-YKSNMDHNSSLDQP 1483
D. persimilis 1445 ------QEDATTPLRVGDYQG-YKSNMDHNSSLDQP 1473
D. willistoni 1514 QDH----EDATTPLRVGDYQSGYKSNMDQNASLEQP 1545
D. mojavensis 1355 ADG----EDATTPLRVGEYQG-YKSNMDHNTSLEQP 1385
D. virilis 1414 VDG----EDATTPLRVGEYEG-YKSNMEHNESVEQP 1444
D. grimshawi 1384 VDG----EDATTPLRVGEYQG-YKSNMEHNTSMDQP 1414

D

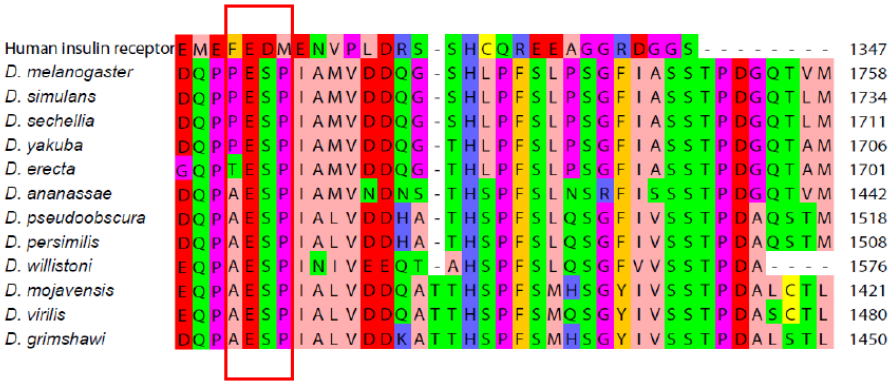
Human insulin receptor EMEFEDMENVPLDRS-SHCQREEAGGRDGGS 1347
D. melanogaster DQPPESPIAMVDDQG-SHLPFSLPSGFIASSTPDGQTVM 1758
D. simulans DQPPESPIAMVDDQG-SHLPFSLPSGFIASSTPDGQTLM 1734
D. sechellia DQPPESPIAMVDDQG-SHLPFSLPSGFIASSTPDGQTLM 1711
D. yakuba DQPPESPIAMVDDQG-THLPFSLPSGFIASSTPDGQTAM 1706
D. erecta GQPTESPIAMVDDQG-THLPFSLPSGFIASSTPDGQTAM 1701
D. ananassae DQPAESPIAMVNDNS-THSPFSLNSRFISSSTPDGQTVM 1442
D. pseudoobscura DQPAESPIALVDDHA-THSPFSLQSGFIVSSTPDAQSTM 1518
D. persimilis DQPAESPIALVDDHA-THSPFSLQSGFIVSSTPDAQSTM 1508
D. willistoni EQPAESPINIVEEQT-AHSPFSLQSGFVVSSTPDA---- 1576
D. mojavensis EQPAESPIALVDDQATTHSPFSMHSGYIVSSTPDALCTL 1421
D. virilis EQPAESPIALVDDQATTHSPFSMQSGYIVSSTPDASCTL 1480
D. grimshawi DQPAESPIALVDDKATTHSPFSMHSGYIVSSTPDALSTL 1450

E

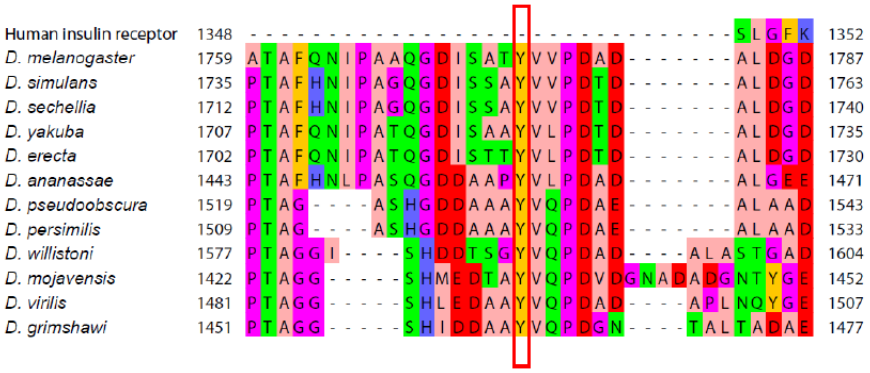
Human insulin receptor 1348 ----------SLGFK 1352
D. melanogaster 1759 ATAFQNIPAAQGDISATYVVPDAD-------ALDGD 1787
D. simulans 1735 PTAFHNIPAGQGDISSAYVVPDTD-------ALDGD 1763
D. sechellia 1712 PTAFHNIPAGQGDISSAYVVPDTD-------ALDGD 1740
D. yakuba 1707 PTAFQNIPATQGDISAAYVLPDTD-------ALDGD 1735
D. erecta 1702 PTAFQNIPATQGDISTTYVLPDTD-------ALDGD 1730
D. ananassae 1443 PTAFHNLPASQGDDAAPYVLPDAD-------ALGEE 1471
D. pseudoobscura 1519 PTAG----ASHGDDAAAYVQPDAE-------ALAAD 1543
D. persimilis 1509 PTAG----ASHGDDAAAYVQPDAE-------ALAAD 1533
D. willistoni 1577 PTAGGI----SHDDTSGYVQPDAD----ALASTGAD 1604
D. mojavensis 1422 PTAGG-----SHMEDTAYVQPDVDGNADADGNTYGE 1452
D. virilis 1481 PTAGG-----SHLEDAAYVQPDAD----APLNQYGE 1507
D. grimshawi 1451 PTAGG-----SHIDDAAYVQPDGN----TALTADAE 1477

F

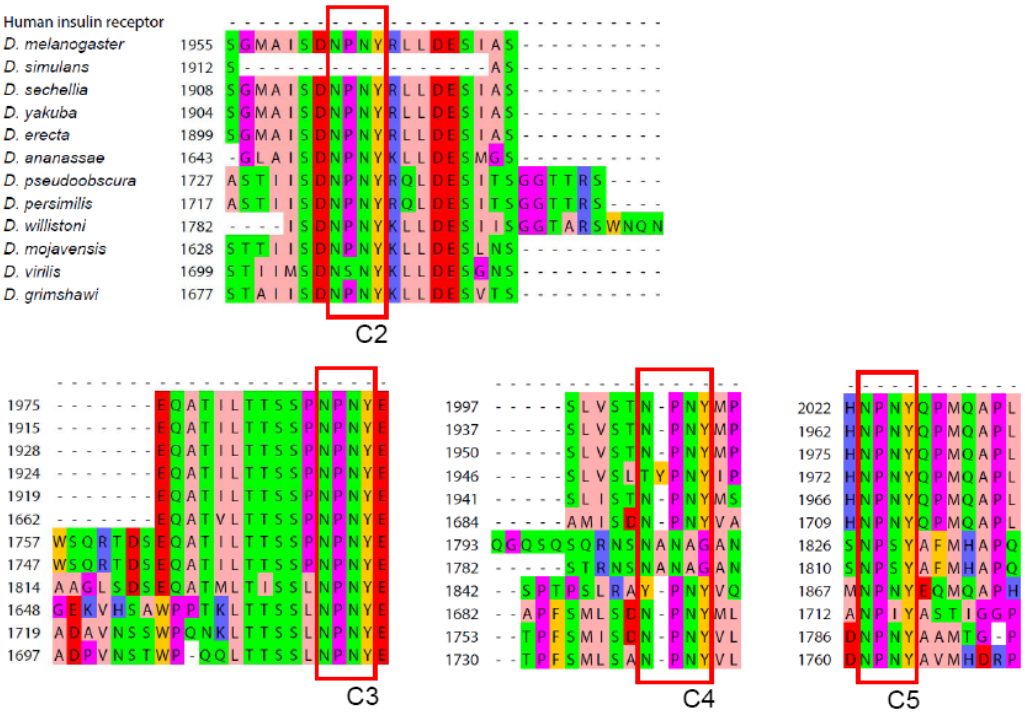
Human insulin receptor
D. melanogaster 1955
D. simulans 1912
D. sechellia 1908
D. yakuba 1904
D. erecta 1899
D. ananassae 1643
D. pseudoobscura 1727
D. persimilis 1717
D. willistoni 1782
D. mojavensis 1628
D. virilis 1699
D. grimshawi 1677
C2
C3
C4
C5

G

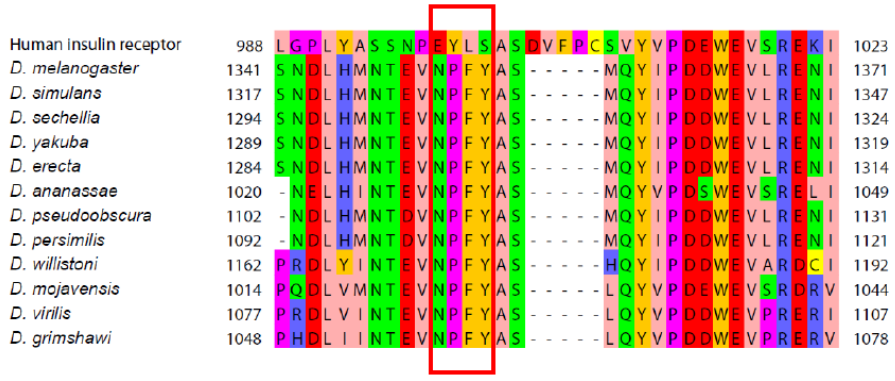
Human insulin receptor 988
D. melanogaster 1341
D. simulans 1317
D. sechellia 1294
D. yakuba 1289
D. erecta 1284
D. ananassae 1020
D. pseudoobscura 1102
D. persimilis 1092
D. willistoni 1162
D. mojavensis 1014
D. virilis 1077
D. grimshawi 1048

H

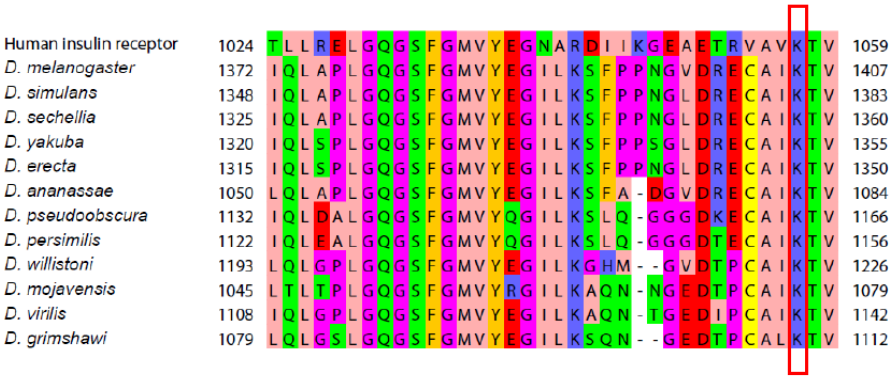

Figure 13. Conservation of selected known and potential interaction sites in the insulin receptor across 12 sequenced *Drosophila* species and in humans. A ClustalW multiple sequence alignment was generated and amino acid residues were colored using the Zappo scheme, in which different colors are used for amino acids with different chemical and physical properties. The coloring scheme is as follows: light pink = aliphatic/hydrophobic; light orange = aromatic; red = positive; green = negative; blue = hydrophilic; fuschia = proline or glycine; yellow = cysteine. Fragments of the multiple sequence alignment are shown. (A) Map of the C-tail and the region upstream that was inadvertently deleted in all ΔA contructs, which were made before my involvement in this project. The blue rectangle outlines the region deleted in the ΔAB construct. (B) The inadvertently deleted region contains two tyrosines that are conserved in all 12 of the

sequenced *Drosophila* species, but not in human IR. The region also contains a PXXP motif that seems weakly conserved among the *Drosophila* species and is not present in human IR. (C) Y1 in the DInR C-tail is conserved among all, except *D. ananassae*, of the sequenced *Drosophila* species. (D) The PXXP motif in region A is conserved in 4 *Drosophila* species. (E) Y2 is conserved in all 12 *Drosophila* species. (F) The NPXY motif containing Y8 (also called C3) is completely conserved in all 12 *Drosophila* species. The NPXY motif containing Y10 (C5) is almost completely conserved, with only some changes in the variable X position. The NPXY motifs containing Y7 (C2) and Y9 (C4) are less well-conserved. (G) The NPXY motif in the juxtamembrane domain of DInR is completely conserved among the 12 *Drosophila* species; the juxtamembrane NPXY motif in human IR, which is an NPEY, is shifted 2 amino acid residues towards the N-terminus in this multiple sequence alignment. (H) The lysine in the kinase domain of DInR that was deleted in the kinase-dead construct is conserved among all 12 sequenced *Drosophila* species and in human IR. Red boxes outline the residues being discussed.

of these motifs, so it remains a possibility that a subset of the four NPXpY motifs in the C-tail are actually responsible for the in vitro binding between Chico and DInR. Poltilove et al. (2000) also showed that the juxtamembrane NPXpY motif was required for the efficient phosphorylation of Chico by DInR in vitro.

A previous postdoctoral fellow in the lab, D. Guo, used the yeast two-hybrid technique to test different potential binding sites in the C-tail of DInR for interaction with Dock. In order to test multiple binding sites at a time, he deleted large regions of the C-tail (Figure 13A). Region A contains Y1 and a PXXP motif (PESP); unfortunately, it was subsequently found that upstream sites were inadvertently included in region A (Figure 13A). When J. Song had deleted the C-tail to show by yeast two-hybrid that it was required for binding between DInR and Dock (Song et al., 2003), the deletion began at the PstI site (Figure 13A), whereas in D. Guo's yeast two-hybrid constructs, the deletion began upstream of the PstI site at the ClaI site (Figure 13A). Thus, an additional two tyrosines and a PXXP motif were inadvertently included in region A. These two tyrosines are conserved in all 12 sequenced *Drosophila* species, but not in the human IR receptor (Figure 13B), suggesting that they might be functionally important in *Drosophila*. The PXXP motif appears to be weakly conserved among the 12 sequenced *Drosophila* species and is absent in the human IR (Figure 13B).

Region B contains Y2, 3, and 4. Region C contains Y5 to 10; Y7, 8, 9, and 10 are located in NPXpY motifs. Region D contains the PTNP and PPPP motifs. Figure 13 shows the conservation of some of these potential binding sites in the 12 sequenced *Drosophila* species and in the human IR. In yeast two-hybrid assays,

deletion of regions A and B together abolished binding between DInR and Dock (Figure 14). Neither region A alone nor region B alone were sufficient for interaction between DInR and Dock. The deletion of regions C and D did not decrease binding.

Individual potential binding sites were also tested by D. Guo by site directed mutagenesis to change specific tyrosine residues to phenylalanine. The mutation of Y1 (in region A) did not affect binding (Figure 14). At the time (before it was found that upstream sites were inadvertently included in region A), this indirectly implicated the PESP motif as being responsible for the requirement of region A for binding since it was the only other motif in region A (Figure 14). When Y2 (in region B) was changed to phenylalanine, there was a drastic reduction in binding. When the other two potential binding sites in region B, Y3 and Y4, were mutated in combination, there was no effect on binding. Thus, it was concluded that the PESP and Y2 sites of DInR were the putative Dock binding sites. However, the recent realization that upstream sites were included in region A raises doubt about the PESP requirement for binding (see above).

6.2 Experimental design

The in vitro studies by Poltilove et al. (2000) and D. Guo (summarized above) showed which motifs were important for interaction between DInR and Chico, or between DInR and Dock, respectively. However, these in vitro studies are only suggestive, as protein-protein interactions in vivo may be influenced by the cellular environments in which the proteins are endogenously expressed. They further cannot provide evidence that the motifs are required for specific functions of DInR in growth

A

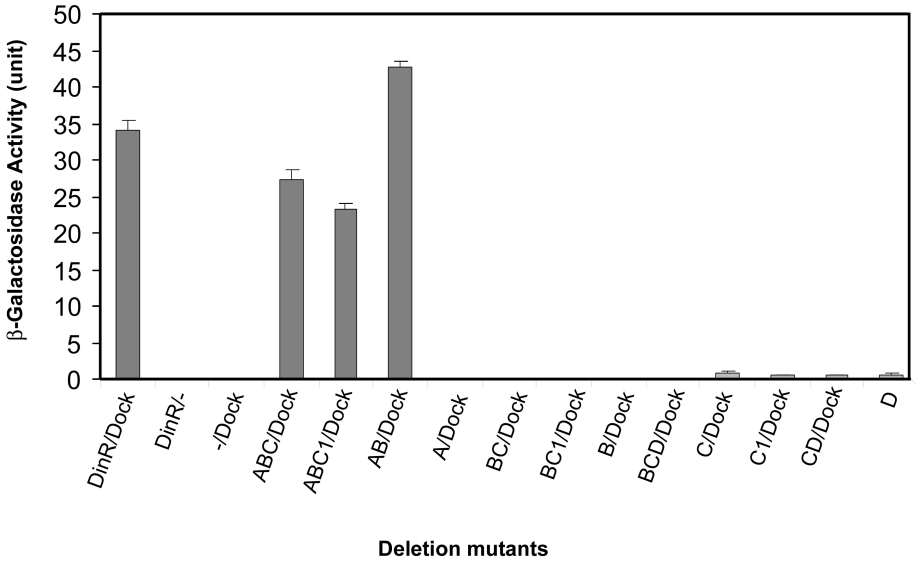

D. Guo, unpublished

B

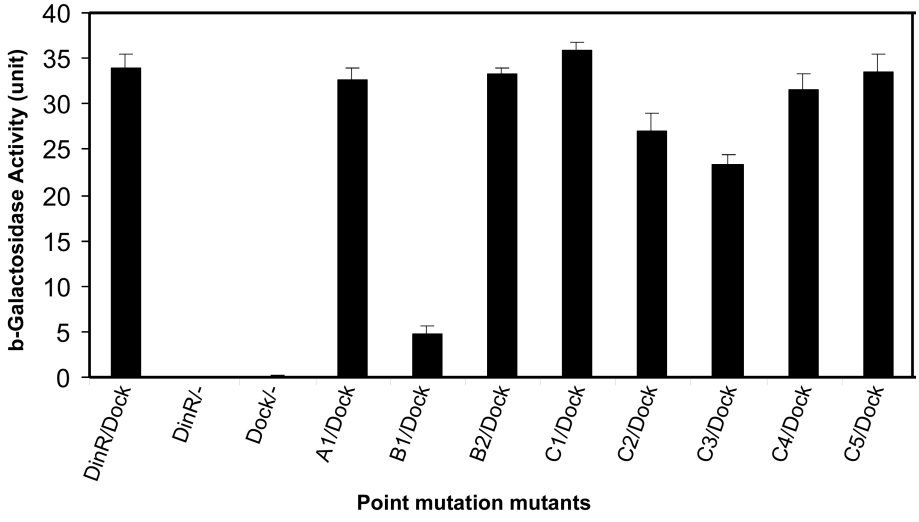

D. Guo, unpublished

Figure 14. Identification of sites on DInR that are required for binding to Dock. (A) Various deletion constructs of DInR were tested by yeast two-hybrid for their ability to bind Dock. Deletion of regions C and D together did not decrease binding to Dock (AB/Dock), as compared to the control (DinR/Dock). Deletion of region A in addition to regions C and D abolished binding to Dock (B/Dock). Deletion of region B in addition to regions C and D also abolished interaction with Dock (A/Dock). (B) Individual potential binding sites on DInR were mutated in order to test their requirement for Dock binding. Mutation of the first tyrosine in region B of DInR severely decreased binding to Dock (B1/Dock). This experiment was designed and performed by D. Guo.

control through Chico or axon guidance through Dock. Although in vitro explant or cell culture experiments could provide such evidence, we reasoned that in vivo experiments, which are feasible using the many genetic techniques and assays that have been developed for the *Drosophila melanogaster* model system, would provide the most convincing evidence since the natural developmental and physiological milieu would be present.

For our experimental approach, we used the GAL4/UAS system developed by Brand and Perrimon (1993). This system allows targeted gene expression in the tissues and developmental stage(s) of the experimenters' choosing. In essence, the expression of the yeast GAL4 transcription factor is directed by a *Drosophila* regulatory element. GAL4 will bind to its upstream activating sequence (UAS) and drive expression of the desired gene product, the sequence of which has been placed downstream of the UAS. For our experiments, we used the *arm-GAL4* driver (Sanson et al., 1996), which drives expression ubiquitously during multiple stages of development, and have placed *dinr* constructs with various deletions or point mutations downstream of the UAS (Materials and Methods). A full-length *dinr* contruct was used as the positive control. *UAS-lacZ* was used as the negative control.

The experimental design was to add back the mutant DInR being tested to the *dinr* mutant background. For my experiments, I used the $dinr^{ex15/273}$ mutant background. The $dinr^{ex15/273}$ transheterozygotes carry one copy of the $dinr^{ex15}$ null allele and one copy of the $dinr^{273}$ weak hypomorphic allele. Although using the $dinr^{ex15/ex15}$ mutant background would have been a "cleaner" background to use, I was

unable to rescue the adult lethality of this mutant using several control *dinr* constructs that I tested.

D. Guo cloned *dinr*, made a full-length Myc-tagged *UAS-dinr* construct, and subcloned the following Myc-tagged mutant *dinr* constructs: *UAS-dinr(KA), UAS-dinr(Y1F), UAS-dinr(Y2F), UAS-dinr(Y1F,Y2F), UAS-dinr(PESP→LESL), UAS-dinr(LESL,Y2F), UAS-dinr(Y7F), UAS-dinr(Y8F), UAS-dinr(Y9F), UAS-dinr(Y10F), UAS-dinr(Y7,8,9,10F), UAS-dinr(ΔAB), UAS-dinr(ΔABC),* and *UAS-dinr(ΔCD)*. When I became involved in this project, my first task was to subclone these three Myc-tagged mutant *dinr* constructs: *UAS-dinr(ΔC-tail), UAS-dinr(JM-NPFF),* and *UAS-dinr(5NPXF).* As I was in the process of subcloning the *UAS-dinr(ΔC-tail)* construct, it became apparent that the sequence defined as being part of "region A" included a region upstream of the start of the C-tail. Thus, all the constructs where region A was deleted, including my *ΔC-tail* construct, which I finished subcloning but did not test in the rescue experiments, were missing potential binding sites upstream of the C-tail.

The main predictions of the rescue experiments were that transgenes carrying mutations in Chico binding and/or interaction sites (since the juxtamembrane NPFY motif was shown by Poltilove et al. (2000) to be required for the efficient phosphorylation of Chico by DInR) would 1) fail to rescue growth defects, but 2) allow rescue of axon guidance defects. In contrast, transgenes carrying mutations in Dock binding sites would 3) allow rescue of growth defects, and 4) fail to rescue axon guidance defects.

The genetic crossing scheme to generate the stocks to be used for the rescue experiments is described in the Materials and Methods section. Some flies generated during the crossing scheme were sickly and I was unable to generate the final stocks for the respective transgenic constructs. Also, some final stocks were very difficult to maintain and died out completely and unexpectedly.

The cross for the experiments to test rescue of the lethality and growth defect of $dinr^{ex15/273}$ transheterozygotes was as follows (*UAS-X* represents the *dinr* control or mutant transgene being tested):

$$\frac{armGAL4}{armGAL4}\,;\,\frac{FRT82Bdinr^{273}}{TM3Sb,armGFP}\ \text{virgin}\ \female\ \times\ \frac{UAS\text{-}X}{UAS\text{-}X\ (\text{or}\ CyO)}\,;\,\frac{dinr^{ex15}}{TM3Sb,armGFP}\ \male$$

The possible genotypes and phenotypes from this cross are as follows. Note that flies carrying 2 copies of the *TM3Sb,armGFP* balancer are lethal.

1) $; \frac{armGAL4}{UAS\text{-}X}\,;\,\frac{FRT82Bdinr^{273}}{dinr^{ex15}}$	non-Sb phenotype
2) $; \frac{armGAL4}{UAS\text{-}X}\,;\,\frac{FRT82Bdinr^{273}}{TM3,armGFP}$	Sb phenotype because of the presence of the third chromosome balancer
3) $; \frac{armGAL4}{UAS\text{-}X}\,;\,\frac{dinr^{ex15}}{TM3,armGFP}$	Sb phenotype because of the presence of the third chromosome balancer

If each of the above genotypes were fully viable, then each would comprise 33% of the total progeny population. Adult flies of the genotype $FRT82Bdinr^{273}/dinr^{ex15}$ are usually adult lethal; if this lethality was fully rescued by the *UAS-X* transgene being tested, then 33% of the total progeny would be non-Sb.

For each *UAS-X* transgene tested, the ability to rescue adult lethality was determined. If adult lethality was rescued, then the rescue of growth defects in adults was possible to assess.

The cross for the experiments to test for rescue of the photoreceptor axon guidance defects of $dinr^{ex15/273}$ transheterozygotes was similar to the above, except that the 3rd-chromosome balancer used was *TM6BTb,GFP*, which is marked with *Tb* and GFP to allow for selection of larvae. $FRT82Bdinr^{273}/dinr^{ex15}$ larvae would be non-Tb and GFP-negative.

6.3 Results

6.3.1 Binding sites important for viability

As expected, the negative control, *UAS-lacZ,* completely failed to rescue the adult lethality of the $dinr^{ex15/273}$ transheterozygotes, yielding 0% adults that were non-Sb (Table 1). Similarly, *UAS-dinr(KA)*, which is a kinase-dead version of *dinr*, failed to rescue, demonstrating that DInR kinase activity is necessary for in vivo function. Also as expected, the wild type *UAS-dinr* transgene completely rescued adult lethality, yielding 37% adults that were non-Sb (Table 1). Mutations that completely failed to rescue lethality, and thus indicate that the mutated sites are important for viability, were: Y1F, ΔAB (two lines tested), and ΔABC. Since Y1 is situated in region A, the absence of Y1 in the transgenes containing ΔAB and ΔABC likely accounts for their failure to rescue lethality. Mutations that partially rescued lethality, and thus indicate that the mutated sites are less important for viability, were: Y9F, Y7,8,9,10F (each of the mutated tyrosines are in the NPXY motifs of the C-tail),

Table 1. Ability of *UAS-dinr* proteins to rescue the adult lethality of *dinr*$^{ex15/273}$ mutant transheterozygotes.

Rescue construct	% that were non-Sb (viable *dinr*$^{ex15/273}$ adults)	% that were Sb (viable *dinr*$^{ex15/+}$ or *dinr*$^{273/+}$ adults)	Total # of flies scored
UAS-lacZ	0	100	237
UAS-dinr	37	63	785
UAS-dinr(KA)	0	100	34
UAS-dinr(Y1F)	0	100	245
UAS-dinr(Y2F)	8	92	153
UAS-dinr(Y1F,Y2F)	(11)	(89)	(9)
UAS-dinr(LESL)	42	58	177
UAS-dinr(LESL,Y2F)	11	89	254
UAS-dinr(ΔAB) #1	0	100	130
UAS-dinr(ΔAB) #2	0	100	112
UAS-dinr(ΔABC)	0	100	74
UAS-dinr(JM-NPFF) #1	32	68	73
UAS-dinr(JM-NPFF) #2	21	79	140
UAS-dinr(Y9)	16	84	145
UAS-dinr(Y7,8,9,10F)	11	89	235
UAS-dinr(ΔCD)	27	73	271
UAS-dinr(5NPXF)	21	79	246

LESL and Y2F together (both putative Dock binding sites), 5NPXF (the mutated tyrosines were in the juxtamembrane NPXY motif and the four NPXY motifs in the C-tail), *ΔCD* (which lacks the 4 NPXY motifs in addition to two other tyrosines and two PXXP sites), and JM-NPFF (in which the tyrosine in the juxtamembrane NPXY motif was mutated). Partial rescue of lethality was seen for one of the two JM-NPFF lines, line #2. In contrast, line #1 fully rescued lethality. This discrepancy that was seen between the two lines may be because the transgenes containing the constructs inserted in different regions of the genome and thus might be expressed at different levels despite using the same GAL4 driver to drive their expression levels. However, expression levels of the two JM-NPFF lines were assayed and found to be similar (Figure 16). The LESL mutation (of one of the putative Dock binding sites, the PESP site) rescued lethality to a greater extent than the expected theoretical percentage. Not enough flies could be assessed for the *UAS-dinr(Y1F,Y2F)* rescue construct (Table 1). However, since the results indicated that the construct containing the Y1F mutation completely failed to rescue lethality, the Y1F,Y2F double mutant construct would not have been expected to be informative anyway. Strangely though, one out of the nine progeny was viable.

6.3.2 Binding sites important for growth control

Compared to the control *UAS-dinr* rescue construct, the mean mass of adult males was not appreciably decreased by the mutation or deletion of the following sites in the mutant *UAS-dinr* rescue constructs: PESP in region A; Y2; PESP and Y2 together; JM-NPFY (line #1); Y9; Y10; Y7,8,9,10; and region CD (Figure 15A).

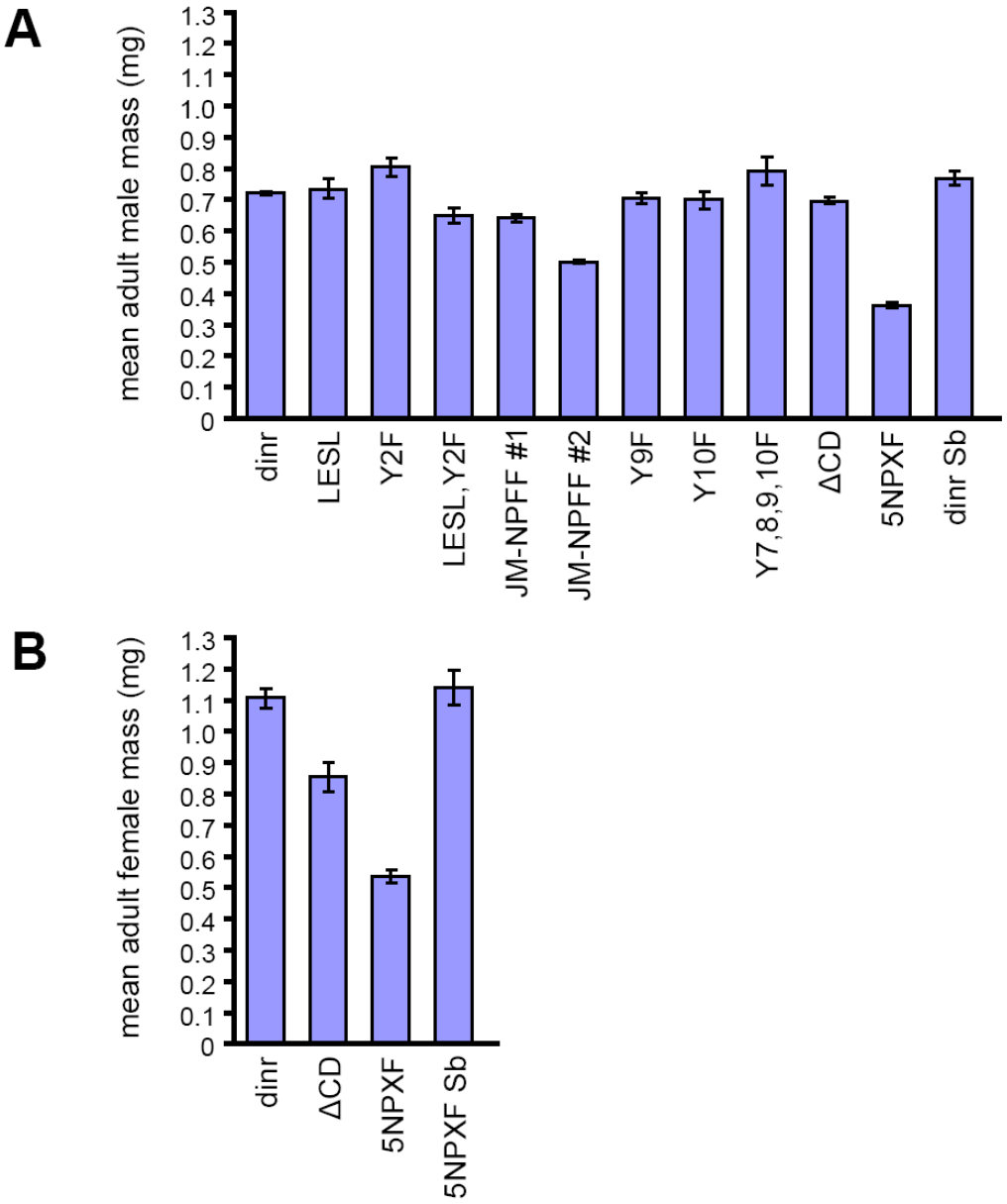

Figure 15. Candidate binding sites in the DInR C-tail are required for whole animal growth control. Mean mass (mg) of male (A) and female (B) adult *dinr*$^{ex15/273}$ flies expressing different *UAS-dinr* constructs. Error bars represent standard error. Sample numbers for

each rescue construct tested in males were: *dinr* control, 85; *dinr(LESL),* 10; *dinr(Y2F)*, 5; *dinr(LESL,Y2F)*, 4; *dinr(JM-NPFF)* #1, 11; *dinr(JM-NPFF)* #2, 22; *dinr(Y9F)*, 10; *dinr(Y10F)*, 5; *dinr(Y7,8,9,10F)*, 2; *dinr(ΔCD)*, 27; *dinr(5NPXF)*, 24; *dinr* control expressed in *dinr* mutant heterozygote siblings (labeled "dinr Sb"), 4. Sample numbers for each rescue construct tested in females were: *dinr* control, 32; *dinr(ΔCD)*, 8; *dinr(5NPXF)*, 9; *dinr(5NPXF)* expressed in *dinr* mutant heterozygote siblings (labeled "5NPXF Sb"), 3.

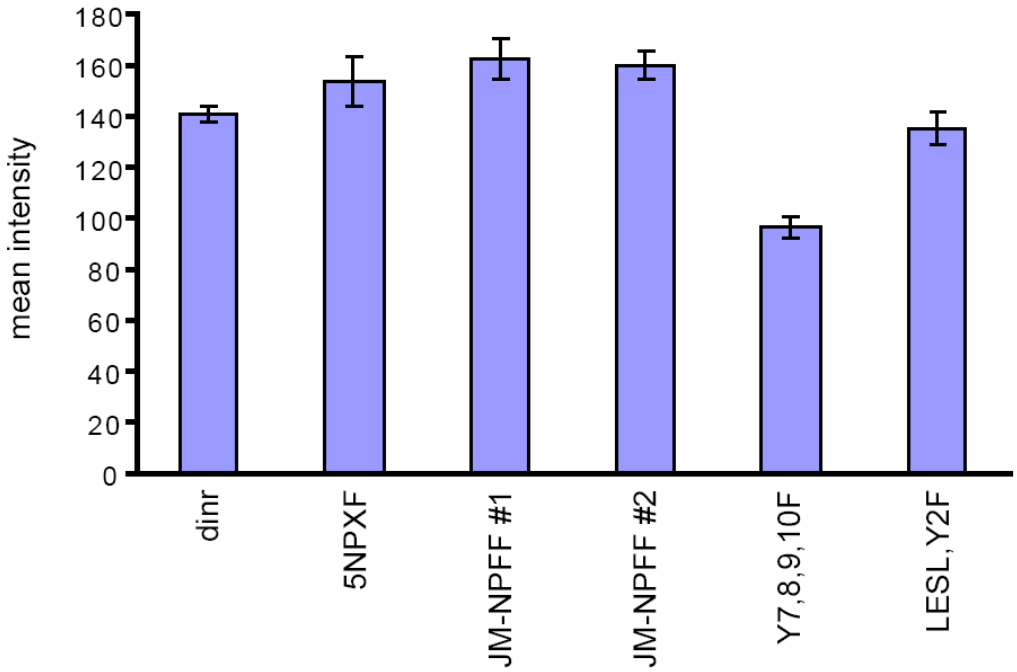

Figure 16. Analysis of expression levels of selected *UAS-dinr* control and mutant transgenes. The Myc-tagged *dinr* transgenes were expressed ubiquitously using the *arm-GAL4* driver. Embryos expressing the transgenes were stained with an anti-Myc antibody and a fluorescently labeled secondary antibody. Mean levels of fluorescence intensity in photographed embryos were measured in Adobe Photoshop. Error bars indicate standard errors.

Unlike line #1 for the *UAS-dinr(JM-NPFF)* construct, line #2 of the same construct led to a sizable decrease in mean male mass (Figure 15A). As was seen for the rescue of lethality, line #2 gave weaker rescue of growth defects than line #1.

There was a 50% decrease in the mean mass of adult males rescued by the *UAS-dinr(5NPXF)* construct compared to those rescued by the control *UAS-dinr* construct (Figure 15A). This decrease is very similar to the 55% decrease in body weight seen in *chico* mutant males (Bohni et al., 1999). Thus, it seems likely that the 5 NPXY sites are responsible for most, if not all, of the control of growth by DInR that is mediated by Chico.

In females, there was a 52% decrease in the mean mass of adult females rescued by the *UAS-dinr(5NPXF)* construct compared to those rescued by the control *UAS-dinr* construct (Figure 15B). This was noticeably less than the 65% decrease in body weight measured in *chico* mutant females (Bohni et al., 1999). Interestingly, although the *UAS-dinr(ΔCD)* construct, which lacks the 4 NPXY sites in the C-tail in addition to 2 tyrosines and 2 PXXP sites, rescued the mean mass of adult males to the same level as the control *UAS-dinr* construct, this did not occur for adult females; instead, there was a 23% decrease in mean mass in females rescued by the *UAS-dinr(ΔCD)* construct (Figure 15B). Thus, it is possible that another interaction site(s) in regions C and D, other than the 4 NPXY sites, may also be responsible for growth control through Chico in females. Since DInR is also involved in controlling female fertility (reviewed in Garofalo, 2002), an interplay between fertility and growth may be at work.

Since it could be argued that the growth decrease in adult flies rescued by *UAS-dinr(5NPXF)* could be due to low expression of the transgene, the expression level of the transgene was measured and was found, in fact, to be comparable to the expression level of the control *UAS-dinr* transgene (Figure 16). Furthermore, the *UAS-dinr(Y7,8,9,10F)* transgene, which completely rescued growth, had a much lower expression level than the control *UAS-dinr* transgene (Figure 16).

6.3.3 Binding sites tested for involvement in R-cell axon guidance control

Although J. Song generated the $dinr^{ex15}$ null allele (Song et al, 2003), he did not test whether it was viable in a heteroallelic combination with a weaker *dinr* allele. I tried raising $dinr^{ex15/273}$ transheterozygotes and found that they were viable at least to the third-instar larval stage – although they were severely developmentally delayed and smaller than WT – and so it was possible to assess photoreceptor axon guidance in these mutants. There was a gross disorganization of the photoreceptor axon targeting in both the lamina and medulla (Figure 17C,D). Clumps of axons were present above and in the lamina, and in the medulla. In general, the phenotypes in the $dinr^{ex15/273}$ eye-brain complexes (Figure 17C,D) seem to be more severe than those of $dinr^{353/273}$ (Song et al., 2003). This is consistent with $dinr^{ex15}$ being a stronger loss-of-function allele than $dinr^{353}$. Since $dinr^{ex15/273}$ transheterozygotes are the *dinr* mutants with the strongest known photoreceptor axon guidance phenotype, these transheterozygotes were chosen as the genetic background to be used for the photoreceptor axon guidance rescue experiments.

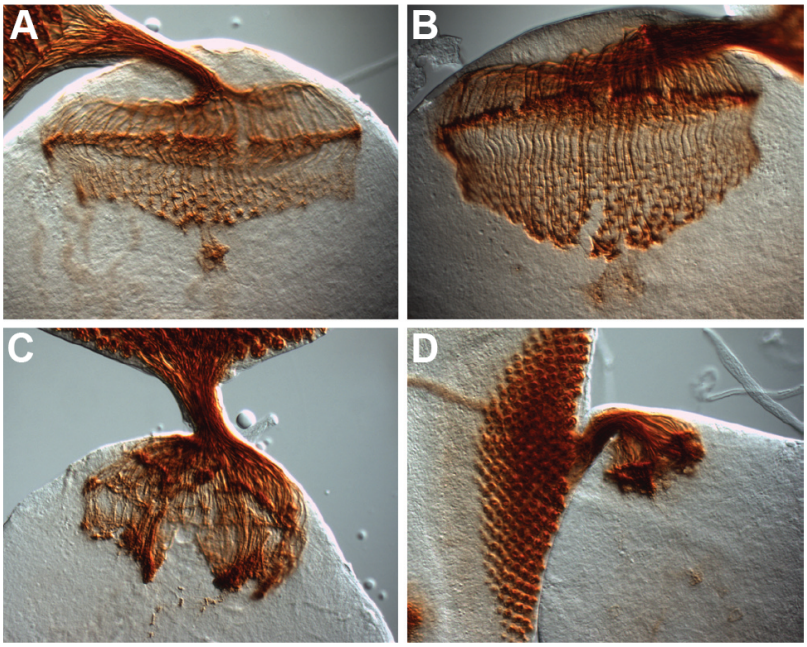

Figure 17. *dinr*$^{ex15/273}$ transheterozygote photoreceptor axon guidance phenotype. Third-instar larval eye-brain complexes were stained with MAb24B10 in order to visualize differentiated photoreceptors and their axons. Imaging was done with DIC optics and a 40× objective. (A, B) Control eye-brain complexes of the genotype w^{1118}. The specimen shown in (B) is at a later stage of development than that shown in (A). The rip in the medulla in (B) resulted during sample preparation. (C, D) *dinr*$^{ex15/273}$ transheterozygote eye-brain complexes.

For all of the rescue constructs tested: the control *UAS-dinr* construct, *UAS-dinr(LESL)*, in which one of the putative Dock binding sites was mutated, *UAS-dinr(Y2F)*, in which the second putative Dock binding site was mutated, *UAS-dinr(LESL,Y2F)*, in which both putative Dock binding sites were mutated, and *UAS-dinr(5NPXF)*, which was hypothesized to only affect growth and not axon guidance, photoreceptor axon guidance appeared relatively normal (Figure 18A-E).

6.4 Discussion

The experiments described here were conducted in order to understand better how a highly pleiotropic gene, *dinr*, is involved in a highly precise developmental process, namely photoreceptor axon guidance, and other processes such as viability and growth. The mutation of the PESP site in region B did not decrease viability. The mutation of Y1 led to complete lethality, whereas the mutation of Y9 alone, Y7,8,9,10 (which are each in NPXY motifs) together, Y7,8,9,10 and the juxtamembrane NPXY motif together, and the juxtamembrane NPXY motif only (which was seen for only one of the two lines) led to partial lethality. Since all of the potential binding sites for downstream signaling proteins were not tested for their requirement for viability, it is possible that other required sites exist.

The mutation of the 5NPXY sites led to a severe decrease in the mean mass of adult males and likely accounts for most, if not all, of the Chico-mediated control of growth by DInR. Although the mutation of the 5NPXY sites also severely decreased the mean mass of adult females, this decrease does not completely account for the decrease in body weight seen in *chico* mutant females. Since the deletion of regions C

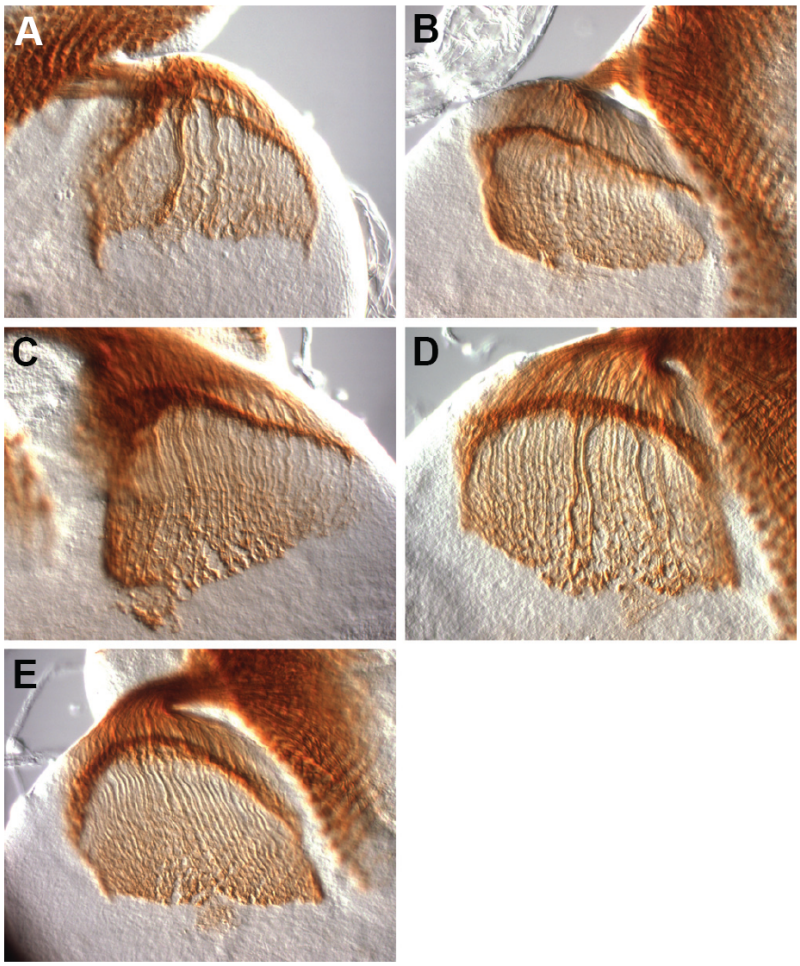

Figure 18. Photoreceptor axon guidance was not disrupted when putative Dock binding sites were mutated individually or in combination. Third-instar larval eye-brain complexes were stained with MAb24B10 and imaged with DIC optics and a 40× objective. Shown is the rescue of the axon guidance defects of the *dinr*$^{ex15/273}$ background with the following constructs: (A) *UAS-dinr* control; (B) *UAS-dinr(LESL)*; (C) *UAS-dinr(Y2F)*; (D) *UAS-dinr(LESL,Y2F)*; (E) *UAS-dinr(5NPXF)*.

and D together led to a noticeable decrease in mean mass, there might be another binding site(s) in these regions that is also important for growth control in females.

Mutating the two putative Dock binding sites individually (Figure 18B,C) or in combination (Figure 18D) did not disrupt R-cell axon guidance . It is possible that another site(s) exists that must be mutated along with the two putative Dock binding sites in order to affect axon guidance. These sites could be the two tyrosines or the PXXP motif upstream of the C-tail that were inadvertently deleted in the ΔA constructs, since the deletion of this upstream region and region A together abolished binding between DInR and Dock in D. Guo's yeast two-hybrid experiments (Figure 14). The PESP motif that was thought to account for region A's requirement in binding is only conserved in 4 of the 12 sequenced *Drosophila* species (Figure 13D), while the Y2 motif that likely accounts for region B's requirement in binding is conserved in all 12 of the *Drosophila* species (Figure 13E). The two tyrosines that were inadvertently deleted are conserved in all 12 of the *Drosophila* species (Figure 13B), so they likely explain region A's requirement for binding; the PXXP motif that was also inadvertently deleted is only weakly conserved (Figure 13B). An alternative possibility is that the other two tyrosines in region B, Y3 and Y4, might act redundantly with Y2 and/or the PESP motif in region A in order to control photoreceptor axon guidance. An experiment that would indicate whether autophosphorylated tyrosines on DInR are actually required for photoreceptor axon guidance control would be to test whether the *UAS-dinr(KA)* construct, which lacks kinase activity, can rescue the photoreceptor axon guidance defects of *dinr* mutant transheterozygotes. If there is failure to rescue, this would suggest that another

tyrosine residue, in addition to Y2, must be autophosphorylated for proper photoreceptor axon guidance to occur. However, if there is rescue, then this would suggest that no tyrosines are required, and also that more than one PXXP site, since mutation of only the PESP site had no effect on photoreceptor axon guidance, act redundantly in photoreceptor axon guidance.

None of the constructs containing ΔA in combination with another deletion (a fly line containing a construct with ΔA alone had not been generated) rescued viability in the in vivo rescue experiment. This can be explained by the absence in these constructs of Y1, which was shown to be required for viability. However, the sites upstream of the C-tail that were inadvertantly removed in these constructs might also be required for viability. Furthermore, it is possible that the same potential binding motifs that are required for viability are also required later in development for proper R-cell axon guidance. In order to test this, one would need to provide a rescue construct containing the unmutated binding motif, that is hypothesized to be required for viability and R-cell axon guidance, during earlier development in order to allow viability to the stage when R-cell axon guidance occurs, at which time, one would need to switch to providing a rescue construct containing the mutated binding site to see whether there are disruptive effects on R-cell axon guidance. A single system to drive the expression of two different transgenic constructs during different developmental stages of a single organism is not yet available for the *Drosophila* model system. However, one could try using the temperature-sensitive GAL80 system, in which the GAL80 molecule is a repressor of GAL4 at permissive temperatures (reviewed in McGuire et al., 2004), to control the expression of one of

the constructs (e.g. the unmutated construct) and use the hormone-inducible Gene-Switch system (reviewed in McGuire et al., 2004) to control the expression of the other construct (e.g. the mutated construct). An alternative approach would be to mutate the binding motif directly by homologous recombination (reviewed in Rong, 2002), a technique that has recently become more widely used for *Drosophila* studies. Then one could rescue viability during earlier development by providing the full-length, unmutated DInR rescue construct either by using 1) a GAL4 driver that drives expression only during earlier development, or 2) by using a GAL4 driver that drives expression during all stages of development and by using temperature-sensitive GAL80 to repress the expression of the unmutated DInR rescue construct precisely at the time when one wants to test the binding motif mutation.

Although the binding sites on DInR that control photoreceptor axon guidance were not identified in this study, we did discover that mutation of the five NPXY sites greatly decreased growth, but had no effect on photoreceptor axon guidance. Thus, these results indicate that the sites responsible for growth control are different than the sites responsible for photoreceptor axon guidance control.

Chapter 7: Conclusions and Future Perspectives

7.1 Identifying the ligand(s) for DInR in directing photoreceptor axon guidance

The discovery that DInR is required for proper photoreceptor axon guidance (Song et al., 2003) led to the obvious question of: what ligand activates DInR in order to control this process? The candidate ligands were the seven putative ligands for DInR, *dilps 1-7* (Brogiolo et al., 2001). This hypothesis was tested through gain-of-function and loss-of-function experiments. An unexpected finding of these experiments was that none of the seven *dilps* seem to be necessary for photoreceptor axon guidance. Mutants lacking *dilps 1-5* in combination, or *dilp6* and *dilp7* individually, showed normal overall photoreceptor axon guidance. Mutation of a ligand(s) that acts through DInR in order to control photoreceptor axon guidance would be expected to lead to the same severely disrupted axon guidance phenotype as was seen in *dinr* mutant transheterozygotes.

It remains a possibility that the *dilps* may actually be involved, but that the correct combination of *dilps* was not examined; the largest combination of *dilp* mutations examined was for *dilps 1-5*. As discussed in Chapter 3, it would be worth testing a mutant lacking *dilp1, -4,* and -7 to determine whether these genes regulate photoreceptor axon guidance in a redundant manner. Another possibility is that another molecule actually serves as the ligand. In such a case, biochemical approaches or genetic screens could lead to the identification of the ligand.

7.2 Allometry depends on *dilp1, -2, -3, -4,* and/or *-5*

Allometry was disrupted in the *Df[dilp1-5]* mutant, thus implicating *dilp1, -2, -3, -4,* and/or *-5* in the control of allometry. Examining smaller combinations of these *dilps* would allow the specific *dilp(s)* that controls allometry to be identified. Once the specific *dilp(s)* is identified, genetic interaction or epistasis experiments could be carried out in order to confirm that the *dilp(s)* controls allometry through the DInR and Chico signaling pathway. Furthermore, the five NPXY sites on DInR, which were shown to be required for growth control by DInR (Chapter 6 of this thesis) could be tested for their requirement in controlling allometry, which is a special case of growth control since different body parts grow differently relative to each other or relative to the entire body of the animal (reviewed in Shingelton et al., 2007).

7.3 Developmental delay is not a factor underlying photoreceptor axon guidance defects

Wild type and control eye-brain complexes at an early stage of development displayed photoreceptor axon targeting that was ordered and that did not resemble the disrupted phenotype of the *dinr* mutant transheterozygotes at a later stage of development. Thus, the future study of *dinr* mutant transheterozygotes does not have to take developmental delay into account as a factor underlying these mutants' photoreceptor axon guidance defects.

7.4 Functional dissection of the signaling domains of the *Drosophila* insulin receptor

The panel of *dinr* control and mutant rescue constructs made primarily by D. Guo, and to which I contributed two constructs, allowed the identification of binding sites on DInR important for viability and growth control. Most strikingly for the viability rescue experiments, mutation of Y1, the first tyrosine residue in the C-tail, led to a complete failure to rescue the adult lethality of $dinr^{ex15/273}$ transheterozygotes (Table 1). This suggests that the DInR Y1 site binds to an unidentified adaptor protein or other downstream signaling component. The unidentifed protein is probably not Chico nor Dock because *chico* mutants and *dock* mutants can sometimes survive until adulthood; *chico* mutants are semi-lethal and *dock* mutants are mostly pupal-lethal (Bohni et al., 1999; Garrity et al., 1996). Furthermore, when the DInR Y1 site was mutated, there was no effect on the mutated DInR protein's binding to Dock in a yeast two-hybrid assay (D. Guo, unpublished)(Figure 14), suggesting that the Y1 site is not required for Dock binding to DInR. A number of candidate DInR downstream signaling components other than Dock were identified by J. Song in his yeast two-hybrid screen for proteins that bind the intracellular domain of DInR (J. Song, unpublished). These candidate proteins could be tested by yeast two-hybrid for their ability to bind the DInR protein containing the Y1 site mutation; any proteins that showed a significant reduction in binding could then be tested by in vivo experiments for their requirement for viability. In this way, the downstream signaling pathway responsible for the requirement of DInR for viability could be identified.

In the photoreceptor axon guidance rescue experiments, mutation of both putative Dock binding sites, the PESP site and Y2, individually or in combination, did not severely affect photoreceptor axon guidance (Figure 18B-D). Other sites on DInR may be required for controlling photoreceptor axon guidance, possibly by acting redundantly with the PESP site and/or Y2.

In the growth rescue experiments, the five NPXY sites of DInR were shown to be required for the control of adult male and female growth by DInR (Figure 15). In order to confirm that growth control by the five NPXY sites is mediated through interaction with Chico, genetic interaction or epistasis experiments could be performed. Since the five NPXY sites were found to be dispensable for the control of photoreceptor axon guidance (Figure 18E), this leads us to conclude that DInR controls growth and photoreceptor axon guidance through different interaction sites. This is an important finding since it points to a strategy used by a pleiotropic cell surface receptor to control at least two of its different functions.

The panel of rescue constructs may be used to identify binding sites on DInR important for other developmental and physiological processes known to be controlled by DInR, by its upstream *dilp* ligands, or downstream signaling molecules. These processes include: sugar homeostasis (Belgacem and Martin, 2006), allometry (Shingleton et al., 2005), exit of neural stem cells from quiescence (Chell and Brand, 2010), and female fertility (Chen et al., 1996). It would be interesting to see how much or how little overlap there is in DInR binding site requirements for these various processes.

References

Adams, M. D., Celniker, S. E., Holt, R. A., Evans, C. A., Gocayne, J. D., Amanatides, P. G., Scherer, S. E., Li, P. W., Hoskins, R. A., Galle, R. F.*, et al.* (2000). The genome sequence of Drosophila melanogaster. Science *287*, 2185-2195.

Bailyes, E. M., Shennan, K. I., Seal, A. J., Smeekens, S. P., Steiner, D. F., Hutton, J. C., and Docherty, K. (1992). A member of the eukaryotic subtilisin family (PC3) has the enzymic properties of the type 1 proinsulin-converting endopeptidase. Biochem J *285 (Pt 2)*, 391-394.

Bateman, J. M., and McNeill, H. (2004). Temporal control of differentiation by the insulin receptor/tor pathway in Drosophila. Cell *119*, 87-96.

Belgacem, Y. H., and Martin, J. R. (2006). Disruption of insulin pathways alters trehalose level and abolishes sexual dimorphism in locomotor activity in Drosophila. J Neurobiol *66*, 19-32.

Bennett, D. L., Bailyes, E. M., Nielsen, E., Guest, P. C., Rutherford, N. G., Arden, S. D., and Hutton, J. C. (1992). Identification of the type 2 proinsulin processing endopeptidase as PC2, a member of the eukaryote subtilisin family. J Biol Chem *267*, 15229-15236.

Bohni, R., Riesgo-Escovar, J., Oldham, S., Brogiolo, W., Stocker, H., Andruss, B. F., Beckingham, K., and Hafen, E. (1999). Autonomous control of cell and organ size by CHICO, a Drosophila homolog of vertebrate IRS1-4. Cell *97*, 865-875.

Brand, A. H., and Perrimon, N. (1993). Targeted gene expression as a means of altering cell fates and generating dominant phenotypes. Development *118*, 401-415.

Britton, J. S., and Edgar, B. A. (1998). Environmental control of the cell cycle in Drosophila: nutrition activates mitotic and endoreplicative cells by distinct mechanisms. Development *125*, 2149-2158.

Brogiolo, W., Stocker, H., Ikeya, T., Rintelen, F., Fernandez, R., and Hafen, E. (2001). An evolutionarily conserved function of the Drosophila insulin receptor and insulin-like peptides in growth control. Curr Biol *11*, 213-221.

Broughton, S., Alic, N., Slack, C., Bass, T., Ikeya, T., Vinti, G., Tommasi, A.M., Driege, Y., Hafen, E., and Partridge, L. (2008). Reduction of DILP2 in Drosophila triages a metabolic phenotype from lifespan revealing redundancy and compensation among DILPs. PLoS One *3*, e3721.

Brummer, T., Schmitz-Peiffer, C., and Daly, R. J. (2010). Docking proteins. Febs J *277*, 4356-4369.

Buday, L., Wunderlich, L., and Tamas, P. (2002). The Nck family of adapter proteins: regulators of actin cytoskeleton. Cell Signal *14*, 723-731.

Campanella, J. J., Bitincka, L., and Smalley, J. (2003). MatGAT: an application that generates similarity/identity matrices using protein or DNA sequences. BMC Bioinformatics *4*, 29.

Chell, J. M., and Brand, A. H. (2010). Nutrition-responsive glia control exit of neural stem cells from quiescence. Cell *143*, 1161-1173.

Chen, C., Jack, J., and Garofalo, R. S. (1996). The Drosophila insulin receptor is required for normal growth. Endocrinology *137*, 846-856.

Chiu, S. L., and Cline, H. T. (2010). Insulin receptor signaling in the development of neuronal structure and function. Neural Dev *5*, 7.

Clandinin, T. R., and Zipursky, S. L. (2002). Making connections in the fly visual system. Neuron *35*, 827-841.

Desai, C. J., Garrity, P. A., Keshishian, H., Zipursky, S. L., and Zinn, K. (1999). The Drosophila SH2-SH3 adapter protein Dock is expressed in embryonic axons and facilitates synapse formation by the RP3 motoneuron. Development *126*, 1527-1535.

Dickson, B. J. (2003). Development. Wiring the brain with insulin. Science *300*, 440-441.

Fan, X., Labrador, J. P., Hing, H., and Bashaw, G. J. (2003). Slit stimulation recruits Dock and Pak to the roundabout receptor and increases Rac activity to regulate axon repulsion at the CNS midline. Neuron *40*, 113-127.

Fawcett, J. P., Georgiou, J., Ruston, J., Bladt, F., Sherman, A., Warner, N., Saab, B. J., Scott, R., Roder, J. C., and Pawson, T. (2007). Nck adaptor proteins control the organization of neuronal circuits important for walking. Proc Natl Acad Sci U S A *104*, 20973-20978.

Fernandez-Almonacid, R., and Rosen, O. M. (1987). Structure and ligand specificity of the Drosophila melanogaster insulin receptor. Mol Cell Biol *7*, 2718-2727.

Fernandez, R., Tabarini, D., Azpiazu, N., Frasch, M., and Schlessinger, J. (1995). The Drosophila insulin receptor homolog: a gene essential for embryonic development encodes two receptor isoforms with different signaling potential. Embo J *14*, 3373-3384.

Fujita, S. C., Zipursky, S. L., Benzer, S., Ferrus, A., and Shotwell, S. L. (1982). Monoclonal antibodies against the Drosophila nervous system. Proc Natl Acad Sci U S A *79*, 7929-7933.

Gale, E. A. (2001). The discovery of type 1 diabetes. Diabetes *50*, 217-226.

Garofalo, R. S. (2002). Genetic analysis of insulin signaling in Drosophila. Trends Endocrinol Metab *13*, 156-162.

Garrity, P. A., Rao, Y., Salecker, I., McGlade, J., Pawson, T., and Zipursky, S. L. (1996). Drosophila photoreceptor axon guidance and targeting requires the dreadlocks SH2/SH3 adapter protein. Cell *85*, 639-650.

Geminard, C., Rulifson, E. J., and Leopold, P. (2009). Remote control of insulin secretion by fat cells in Drosophila. Cell Metab *10*, 199-207.

Golic, K. G. (1991). Site-specific recombination between homologous chromosomes in Drosophila. Science *252*, 958-961.

Gorczyca, M., Augart, C., and Budnik, V. (1993). Insulin-like receptor and insulin-like peptide are localized at neuromuscular junctions in Drosophila. J Neurosci *13*, 3692-3704.

Gronke, S., Clarke, D. F., Broughton, S., Andrews, T. D., and Partridge, L. (2010). Molecular evolution and functional characterization of Drosophila insulin-like peptides. PLoS Genet *6*, e1000857.

Hing, H., Xiao, J., Harden, N., Lim, L., and Zipursky, S. L. (1999). Pak functions downstream of Dock to regulate photoreceptor axon guidance in Drosophila. Cell *97*, 853-863.

Howard, P. L., Chia, M. C., Del Rizzo, S., Liu, F. F., and Pawson, T. (2003). Redirecting tyrosine kinase signaling to an apoptotic caspase pathway through chimeric adaptor proteins. Proc Natl Acad Sci U S A *100*, 11267-11272.

Huber, A. B., Kolodkin, A. L., Ginty, D. D., and Cloutier, J. F. (2003). Signaling at the growth cone: ligand-receptor complexes and the control of axon growth and guidance. Annu Rev Neurosci *26*, 509-563.

Ikeya, T., Galic, M., Belawat, P., Nairz, K., and Hafen, E. (2002). Nutrient-dependent expression of insulin-like peptides from neuroendocrine cells in the CNS contributes to growth regulation in Drosophila. Curr Biol *12*, 1293-1300.

Kohanski, R. A. (2002). Insulin Receptor. In Diabetes and Carbohydrate Metabolism. I.D. Goldfine and R.J. Rushakoff, eds. (S. Dartmouth: MDTEXT.COM, INC).

Kunes, S., Wilson, C., and Steller, H. (1993). Independent guidance of retinal axons in the developing visual system of Drosophila. J Neurosci *13*, 752-767.

Lee, C. H., Herman, T., Clandinin, T. R., Lee, R., and Zipursky, S. L. (2001). N-cadherin regulates target specificity in the Drosophila visual system. Neuron *30*, 437-450.

Lee, C. H., Li, W., Nishimura, R., Zhou, M., Batzer, A. G., Myers, M. G., Jr., White, M. F., Schlessinger, J., and Skolnik, E. Y. (1993). Nck associates with the SH2 domain-docking protein IRS-1 in insulin-stimulated cells. Proc Natl Acad Sci U S A *90*, 11713-11717.

Lee, Y. S., and Carthew, R. W. (2003). Making a better RNAi vector for Drosophila: use of intron spacers. Methods *30*, 322-329.

Leiter, E. H. (1997). Carboxypeptidase E and obesity in the mouse. J Endocrinol *155*, 211-214.

Lemmon, M. A., and Schlessinger, J. (2010). Cell signaling by receptor tyrosine kinases. Cell *141*, 1117-1134.

LeRoith, D., Lesniak, M. A., and Roth, J. (1981). Insulin in insects and annelids. Diabetes *30*, 70-76.

Li, W., Fan, J., and Woodley, D. T. (2001). Nck/Dock: an adapter between cell surface receptors and the actin cytoskeleton. Oncogene *20*, 6403-6417.

Mast, J. D., Prakash, S., Chen, P. L., and Clandinin, T. R. (2006). The mechanisms and molecules that connect photoreceptor axons to their targets in Drosophila. Semin Cell Dev Biol *17*, 42-49.

McGuire, S. E., Mao, Z., and Davis, R. L. (2004). Spatiotemporal gene expression targeting with the TARGET and gene-switch systems in Drosophila. Sci STKE *2004*, pl6.

Miklos, G. L., and Rubin, G. M. (1996). The role of the genome project in determining gene function: insights from model organisms. Cell *86*, 521-529.

Murillo-Maldonado, J. M., Sanchez-Chavez, G., Salgado, L. M., Salceda, R., and Riesgo-Escovar, J. R. (2011). Drosophila insulin pathway mutants affect visual physiology and brain function besides growth, lipid, and carbohydrate metabolism. Diabetes *60*, 1632-1636.

Newsome, T. P., Asling, B., and Dickson, B. J. (2000). Analysis of Drosophila photoreceptor axon guidance in eye-specific mosaics. Development *127*, 851-860.

Parks, A. L., Cook, K. R., Belvin, M., Dompe, N. A., Fawcett, R., Huppert, K., Tan, L. R., Winter, C. G., Bogart, K. P., Deal, J. E*., et al.* (2004). Systematic generation of high-resolution deletion coverage of the Drosophila melanogaster genome. Nat Genet *36*, 288-292.

Pawson, T. (2007). Dynamic control of signaling by modular adaptor proteins. Curr Opin Cell Biol *19*, 112-116.

Pawson, T., and Scott, J. D. (1997). Signaling through scaffold, anchoring, and adaptor proteins. Science *278*, 2075-2080.

Pessin, J. E., and Saltiel, A. R. (2000). Signaling pathways in insulin action: molecular targets of insulin resistance. J Clin Invest *106*, 165-169.

Petruzzelli, L., Herrera, R., Arenas-Garcia, R., Fernandez, R., Birnbaum, M. J., and Rosen, O. M. (1986). Isolation of a Drosophila genomic sequence homologous to the kinase domain of the human insulin receptor and detection of the phosphorylated Drosophila receptor with an anti-peptide antibody. Proc Natl Acad Sci U S A *83*, 4710-4714.

Poeck, B., Fischer, S., Gunning, D., Zipursky, S. L., and Salecker, I. (2001). Glial cells mediate target layer selection of retinal axons in the developing visual system of Drosophila. Neuron *29*, 99-113.

Poltilove, R. M., Jacobs, A. R., Haft, C. R., Xu, P., and Taylor, S. I. (2000). Characterization of Drosophila insulin receptor substrate. J Biol Chem *275*, 23346-23354.

Prokop, A., and Meinertzhagen, I. A. (2006). Development and structure of synaptic contacts in Drosophila. Semin Cell Dev Biol *17*, 20-30.

Rajala, R. V., Rajala, A., Brush, R. S., Rotstein, N. P., and Politi, L. E. (2009). Insulin receptor signaling regulates actin cytoskeletal organization in developing photoreceptors. J Neurochem *110*, 1648-1660.

Ramiya, V. K., Maraist, M., Arfors, K. E., Schatz, D. A., Peck, A. B., and Cornelius, J. G. (2000). Reversal of insulin-dependent diabetes using islets generated in vitro from pancreatic stem cells. Nat Med *6*, 278-282.

Rao, Y. (2005). Dissecting Nck/Dock signaling pathways in Drosophila visual system. Int J Biol Sci *1*, 80-86.

Rong, Y. S. (2002). Gene targeting by homologous recombination: a powerful addition to the genetic arsenal for Drosophila geneticists. Biochem Biophys Res Commun *297*, 1-5.

Ruan, W., Pang, P., and Rao, Y. (1999). The SH2/SH3 adaptor protein dock interacts with the Ste20-like kinase misshapen in controlling growth cone motility. Neuron *24*, 595-605.

Ruan, Y., Chen, C., Cao, Y., and Garofalo, R. S. (1995). The Drosophila insulin receptor contains a novel carboxyl-terminal extension likely to play an important role in signal transduction. J Biol Chem *270*, 4236-4243.

Rulifson, E. J., Kim, S. K., and Nusse, R. (2002). Ablation of insulin-producing neurons in flies: growth and diabetic phenotypes. Science *296*, 1118-1120.

Saltiel, A. R., and Kahn, C. R. (2001). Insulin signalling and the regulation of glucose and lipid metabolism. Nature *414*, 799-806.

Sanson, B., White, P., and Vincent, J. P. (1996). Uncoupling cadherin-based adhesion from wingless signalling in Drosophila. Nature *383*, 627-630.

Schmucker, D., Clemens, J. C., Shu, H., Worby, C. A., Xiao, J., Muda, M., Dixon, J. E., and Zipursky, S. L. (2000). Drosophila Dscam is an axon guidance receptor exhibiting extraordinary molecular diversity. Cell *101*, 671-684.

Scolnick, J. A., Cui, K., Duggan, C. D., Xuan, S., Yuan, X. B., Efstratiadis, A., and Ngai, J. (2008). Role of IGF signaling in olfactory sensory map formation and axon guidance. Neuron *57*, 847-857.

Shingleton, A. W., Das, J., Vinicius, L., and Stern, D. L. (2005). The temporal requirements for insulin signaling during development in Drosophila. PLoS Biol *3*, e289.

Shingleton, A. W., Frankino, W. A., Flatt, T., Nijhout, H. F., and Emlen, D. J. (2007). Size and shape: the developmental regulation of static allometry in insects. Bioessays *29*, 536-548.

Shoelson, S. E., and Halban, P. A. (1994). Insulin Biosynthesis and Chemistry. In Joslin's diabetes mellitus 13th edition, C.R. Kahn, ed. (Malvern: Lea & Febiger), pp. 29-44.).

Siekhaus, D. E., and Fuller, R. S. (1999). A role for amontillado, the Drosophila homolog of the neuropeptide precursor processing protease PC2, in triggering hatching behavior. J Neurosci *19*, 6942-6954.

Slack, C., Werz, C., Wieser, D., Alic, N., Foley, A., Stocker, H., Withers, D. J., Thornton, J. M., Hafen, E., and Partridge, L. (2010). Regulation of lifespan, metabolism, and stress responses by the Drosophila SH2B protein, Lnk. PLoS Genet *6*, e1000881.

Slaidina, M., Delanoue, R., Gronke, S., Partridge, L., and Leopold, P. (2009). A Drosophila insulin-like peptide promotes growth during nonfeeding states. Dev Cell *17*, 874-884.

Song, J., Wu, L., Chen, Z., Kohanski, R. A., and Pick, L. (2003). Axons guided by insulin receptor in Drosophila visual system. Science *300*, 502-505.

Steiner, D. F. (1998). The proprotein convertases. Curr Opin Chem Biol *2*, 31-39.

Su, Y. C., Maurel-Zaffran, C., Treisman, J. E., and Skolnik, E. Y. (2000). The Ste20 kinase misshapen regulates both photoreceptor axon targeting and dorsal closure, acting downstream of distinct signals. Mol Cell Biol *20*, 4736-4744.

Tatar, M., Kopelman, A., Epstein, D., Tu, M. P., Yin, C. M., and Garofalo, R. S. (2001). A mutant Drosophila insulin receptor homolog that extends life-span and impairs neuroendocrine function. Science *292*, 107-110.

Tayler, T. D., and Garrity, P. A. (2003). Axon targeting in the Drosophila visual system. Curr Opin Neurobiol *13*, 90-95.

Tessier-Lavigne, M., and Goodman, C. S. (1996). The molecular biology of axon guidance. Science *274*, 1123-1133.

Ting, C. Y., and Lee, C. H. (2007). Visual circuit development in Drosophila. Curr Opin Neurobiol *17*, 65-72.

Van Vactor, D., Jr., Krantz, D. E., Reinke, R., and Zipursky, S. L. (1988). Analysis of mutants in chaoptin, a photoreceptor cell-specific glycoprotein in Drosophila, reveals its role in cellular morphogenesis. Cell *52*, 281-290.

Werz, C., Kohler, K., Hafen, E., and Stocker, H. (2009). The Drosophila SH2B family adaptor Lnk acts in parallel to chico in the insulin signaling pathway. PLoS Genet *5*, e1000596.

White, M. F. (2006). The IRS-signalling system: A network of docking proteins that mediate insulin action. Mol. Cell. Biochem. 182, 3-11.

Xu, T., and Rubin, G. M. (1993). Analysis of genetic mosaics in developing and adult Drosophila tissues. Development *117*, 1223-1237.

Yamaguchi, T., Fernandez, R., and Roth, R. A. (1995). Comparison of the signaling abilities of the Drosophila and human insulin receptors in mammalian cells. Biochemistry *34*, 4962-4968.

Zhang, H., Liu, J., Li, C. R., Momen, B., Kohanski, R. A., and Pick, L. (2009). Deletion of Drosophila insulin-like peptides causes growth defects and metabolic abnormalities. Proc Natl Acad Sci U S A *106*, 19617-19622.